

UNCLASSIFIED

AD NUMBER

ADB000216

LIMITATION CHANGES

TO:

Approved for public release; distribution is unlimited. Document partially illegible.

FROM:

Distribution authorized to U.S. Gov't. agencies only; Test and Evaluation; 11 OCT 1974. Other requests shall be referred to Naval Electronics Laboratory Center, Radio Technology Division, San Diego, CA 92152. Document partially illegible.

AUTHORITY

usnelc ltr, 22 apr 1976

THIS PAGE IS UNCLASSIFIED

**Best  
Available  
Copy**

THIS REPORT HAS BEEN DELIMITED  
AND CLEARED FOR PUBLIC RELEASE  
UNDER DOD DIRECTIVE 5200.20 AND  
NO RESTRICTIONS ARE IMPOSED UPON  
ITS USE AND DISCLOSURE.

DISTRIBUTION STATEMENT A

APPROVED FOR PUBLIC RELEASE;  
DISTRIBUTION UNLIMITED.

Technical Document 359

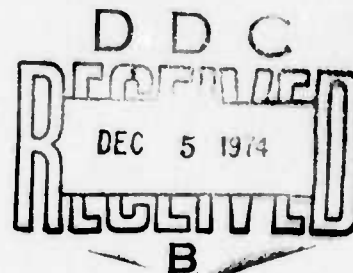
AD B 00216

L

**THIN-WIRE MODELING TECHNIQUES  
APPLIED TO ANTENNA ANALYSIS**

**J. W. Rockway and J. C. Logan  
Radio Technology Division  
( Code 2100 )**

**11 October 1974**



Distribution limited to U. S. Government agencies only;  
Test and Evaluation; 11 October 1974. Other requests for  
this document must be referred to the Naval Electronics  
Laboratory Center.

**NAVAL ELECTRONICS LABORATORY CENTER**

San Diego, California 92152

UNCLASSIFIED

SECURITY CLASSIFICATION OF THIS PAGE (When Data Entered)

REPORT DOCUMENTATION PAGE		READ INSTRUCTIONS BEFORE COMPLETING FORM
1. REPORT NUMBER NELC Technical Document 359 (TD 359)	2. GOVT ACCESSION NO.	3. RECIPIENT'S CATALOG NUMBER
4. TITLE (and Subtitle) THIN-WIRE MODELING TECHNIQUES APPLIED TO ANTENNA ANALYSIS		5. TYPE OF REPORT & PERIOD COVERED
		6. PERFORMING ORG. REPORT NUMBER
7. AUTHOR(s) J. W. Rockway and J. C. Logan		8. CONTRACT OR GRANT NUMBER(s)
9. PERFORMING ORGANIZATION NAME AND ADDRESS Naval Electronics Laboratory Center San Diego, California 92152		10. PROGRAM ELEMENT, PROJECT, TASK AREA & WORK UNIT NUMBERS P 201 (In-House Development Funds)
11. CONTROLLING OFFICE NAME AND ADDRESS Naval Electronics Laboratory Center San Diego, California 92152		12. REPORT DATE 11 October 1974
		13. NUMBER OF PAGES 54
14. MONITORING AGENCY NAME & ADDRESS (if different from Controlling Office)		15. SECURITY CLASS. (of this report) Unclassified
		15a. DECLASSIFICATION/DOWNGRADING SCHEDULE
16. DISTRIBUTION STATEMENT (of this Report) Distribution limited to U. S. Government agencies only; test and evaluation; 11 October 1974. Other requests for this document must be referred to NELC.		
17. DISTRIBUTION STATEMENT (of the abstract entered in Block 20, if different from Report)		
18. SUPPLEMENTARY NOTES		
19. KEY WORDS (Continue on reverse side if necessary and identify by block number) Mathematical models Thin-wire approximations Antenna design Antenna analysis		
20. ABSTRACT (Continue on reverse side if necessary and identify by block number) This document is a summary of work performed in applying thin-wire modeling techniques in support of antenna analysis at NELC during FY74. Detailed discussion is limited to aspects which show how numerical modeling has contributed to an engineering solution. References cited throughout the document provide a source for more complete coverage of a given subject. The first part is intended as an introduction for the uninitiated reader but may prove informative also to those using the same computer codes. The second part describes how thin-wire modeling has been applied to several engineering problems. (CONT)		

DD FORM 1473

1 JAN 73

EDITION OF 1 NOV 65 IS OBSOLETE  
S/N 0102-014-6601

UNCLASSIFIED

SECURITY CLASSIFICATION OF THIS PAGE (When Data Entered)

UNCLASSIFIED

SECURITY CLASSIFICATION OF THIS PAGE(When Data Entered)

(BLOCK 20 CONTINUED)

Thin-wire modeling is demonstrated to be a useful engineering tool in problems involving determination of current distribution, impedance, near- and far-field electric and magnetic components, and efficiency. Listings of the specialized subroutines added by NELC to the AMP program are appended.

UNCLASSIFIED

SECURITY CLASSIFICATION OF THIS PAGE(When Data Entered)

## CONTENTS

1.0	INTRODUCTION . . .	page 1
1.1	THIN-WIRE MODELING TECHNIQUES . . .	1
1.1.1	Thin-wire approximations . . .	1
1.1.2	Method of moments . . .	2
1.2	ELEMENTS OF A GENERAL-PURPOSE PROGRAM . . .	4
1.3	COMPUTER CODES AT NELC . . .	5
1.3.1	AMP . . .	5
1.3.2	SYRACUSE . . .	6
1.3.3	OSU . . .	6
1.3.4	WHIP . . .	6
1.3.5	TWTD . . .	7
1.4	PROGRAM LIMITATIONS . . .	7
1.5	CONFIDENCE FACTORS . . .	7
2.0	SPECIFIC APPLICATIONS . . .	13
2.1	HF ANTENNA SYSTEM DESIGN FOR THE PATROL HYDROFOIL . . .	13
2.1.1	Whip near fields . . .	15
2.1.2	Fan near fields . . .	22
2.1.3	Isolation . . .	23
2.2	MLA-I MINILOOP ANTENNA: A TECHNICAL EVALUATION . . .	24
2.2.1	Efficiency determination . . .	25
2.2.2	Near fields . . .	25
2.2.3	Pattern data . . .	27
2.3	AN/PRC-104 ANTENNA IMPROVEMENT STUDY . . .	29
2.4	EVALUATION OF MULTITURN LOOP ANTENNA . . .	30
2.4.1	Balanced vs unbalanced operation . . .	31
2.4.2	Horizontal vs vertical configuration . . .	33
3.0	CONCLUSIONS . . .	33
	REFERENCES . . .	36
	APPENDIX A: NONRADIATING NETWORK PROGRAM . . .	39
	APPENDIX B: ARC . . .	41
	APPENDIX C: NHFLD, HFK, GH . . .	45
	APPENDIX D: HELIX . . .	49

## ILLUSTRATIONS

- 1 Wire dipole of length  $L$ , radius  $a$  centered about  $z$ -axis . . . page 2
- 2 T-antenna time response to a Gaussian pulse . . . 10
- 3 T-antenna frequency response — real component of input impedance . . . 10
- 4 T-antenna frequency response — reactive component of input impedance . . . 11
- 5 35-foot twin whip over ground plane, dimensions . . . 12
- 6 Scale model of patrol hydrofoil (missile) (PHIM) . . . 14
- 7 Whip on infinite, perfectly conducting ground plane . . . 15
- 8 Peak electric field at various frequencies, case 1 . . . 16
- 9 Peak electric field, 2-15 MHz, case 2 . . . 19
- 10 Comparison of calculated electric near field of whip and sleeve monopole . . . 21
- 11 Comparison of measured and calculated peak electric near fields . . . 21
- 12 Isolation between two 10.67-meter whip antennas spaced 7.6 meters apart over a ground plane . . . 24
- 13 MLA-1 Miniloop installed aboard USS BRADLEY (DE 1041) . . . 25
- 14 Computed values of peak magnetic field strength . . . 26
- 15 Computed values of peak electric field strength . . . 27
- 16 A comparison of the calculated and measured radiation patterns of the MLA-1 Miniloop . . . 28
- 17 HF multiturn loop antenna of Ohio State University . . . 31
- 18 Configurations of balanced and unbalanced MTLs . . . 32
- 19 Horizontal helix with center support . . . 34
- 20 Computed resistance and reactance of horizontal helix with center support . . . 34
- 21 Vertical helix with center support . . . 35
- 22 Computed resistance and reactance of vertical helix with center support . . . 35

## TABLES

- 1 Thin-wire computer codes . . . page 5
- 2 Comparison of T-antenna impedance computations with the measured values of Parsad . . . 9
- 3 Comparison of measurements and computations of a 35-foot twin whip . . . 12
- 4 Comparison of calculated near fields of AMP, SYRACUSE, and WHIP 10.67-meter whip antennas at 2 MHz . . . 22
- 5 Near fields of fan antenna . . . 23
- 6 Efficiencies of inductive-loaded monopoles . . . 29
- 7 Capacitance necessary for resonance for balanced and unbalanced MTL antennas . . . 32

## 1.0 INTRODUCTION

Modern high-speed digital computers and approximate numerical techniques have made possible solutions to many electromagnetic problems which traditionally have been solved only by an empirical approach. An example of a useful type of problem that can be solved numerically is radiation and scattering from thin-wire structures. "Thin-wire modeling" computer programs, when properly used, can be a highly accurate engineering tool for antenna analysis.

This report briefly describes the general approach and applicability of thin-wire modeling programs. Several programs in use at NELC are discussed and compared. Their specific application in support of the analysis of several antenna problems is examined and evaluated. The examples described typify the problems which can be addressed via numerical modeling and demonstrate that numerical modeling is a valuable engineering tool.

This report is a summary of the work performed in applying these numerical modeling techniques during fiscal year 1974. Hence, detailed discussion is limited to those aspects which show how numerical modeling has contributed to an engineering solution. References are cited throughout the report to provide a source for more complete coverage of a given subject. The first part of this report is intended as an introduction for the uninitiated reader but may also prove informative to those currently using the same computer codes. The second part describes how thin-wire modeling techniques have been applied to several engineering problems.

## 1.1 THIN-WIRE MODELING TECHNIQUES

### 1.1.1 THIN-WIRE APPROXIMATIONS

Electromagnetic radiation problems can always be represented by an integral expression with an inhomogeneous source term. The general-purpose programs for frequency domain analysis under discussion here usually approach the thin-wire antenna problem using a Pocklington integral formulation.

The formulation for a z-directed dipole may be written as:<sup>1</sup>

$$E_z^1(z) = \frac{j}{\omega\epsilon} \int_{-L/2}^{L/2} I(z') \left[ \frac{\partial^2 G(z,z')}{\partial z^2} + k^2 G(z,z') \right] dz' \quad (1)$$

where

$$G(z,z') = \frac{\exp(-jkr)}{4\pi r}$$

and  $r$  is the distance between the observation point  $(x, y, z)$  and the source point  $(x', y', z')$ .  $E_z^1(z)$  is the incident or impressed field on the wire, and, since the wire is assumed thin, the field varies only in the direction of the wire. The limits of integration result because the wire dipole extends from  $z = -L/2$  to  $L/2$  as shown in Figure 1. Note that the dipole antenna is not assumed to be infinitely thin. The thin-wire approximations only limit the radius to much less than a wavelength. The approximations also limit the current  $I(z')$  to be only in the axial direction of each wire. Then current and charge densities can be approximated by filaments of current and charge on the wire axes.

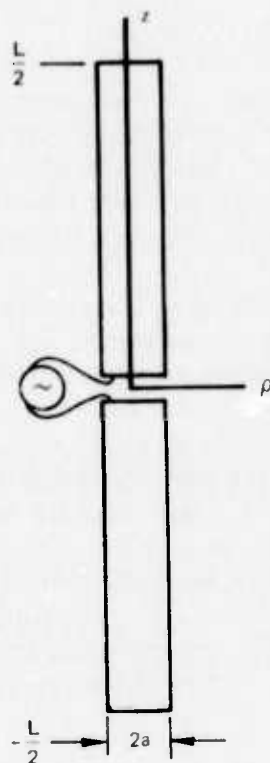


Figure 1. Wire dipole of length  $L$ , radius  $a$  centered about  $z$ -axis.

### 1.1.2 METHOD OF MOMENTS

The unifying concept in this numerical treatment of radiation problems is the method of moments.<sup>2</sup> Basically, the method of moments is a technique for reducing the integral equation (1) to a system of linear algebraic equations where the unknowns are usually coefficients in some appropriate expansion of the current. The resulting matrix equation can then be solved for the current by a high-speed digital computer.

Using the concepts of linear vector spaces and linear operations, equation (1) may be expressed as the operator equation:

$$E_z^I(z) = L(I(z')) \quad (2)$$

where  $E_z^I(z)$  is the known function or source and  $I(z')$  is the unknown current function to be determined. The operator,  $L$ , performs a mapping from one subset containing  $I$  to one containing  $E_z^I$ .

Assuming the wires to be perfect conductors, the boundary condition for the tangential component of the electric field at the wire surface is satisfied (approximately) by requiring that the axial component vanish at the surface of each wire. At points of excitation on the wires of a transmit antenna, some appropriate source model relates an impressed E-field to the excitation voltage.

In a frequently used approach, the subsectional approach, each wire is visualized as divided into a number (N) of short connected segments. A convenient form for the current distribution on each segment is assumed. Thus, the total current along the wire is approximated by an expansion in a series of functions in the domain of L, as:

$$I(z') = \sum_{i=1}^N I_i [g_i(z')] , \quad (3)$$

where  $g_i(z')$  are the expansion functions and  $I_i$  are their coefficients. The problem is to solve for these coefficients.

Substituting equation (3) into equation (2) and using the linearity of L:

$$\sum_{i=1}^N I_i L(g_i(z')) = E_z^I(z) . \quad (4)$$

Equation (4) can be rewritten as a matrix equation by applying a suitably defined inner product and a set of weighting or testing functions (see Reference 2). The inner product of (4) with each testing function,  $t_j$ , is performed, and, since the inner product is a linear operation, the result is:

$$\sum_{i=1}^N I_i \langle t_j, L(g_i(z')) \rangle = \langle t_j, E_z^I(z) \rangle , \quad (5)$$

where  $j = 1, 2, 3, \dots, N$ . Equation (5) can now be written in matrix form as:

$$[Z] [I] = [V] \quad (6)$$

so that

$$[I] = [Z]^{-1} [V] , \quad (7)$$

$$\text{where } [I] = \begin{bmatrix} I_1 \\ I_2 \\ \vdots \\ I_N \end{bmatrix} , \quad (8)$$

$$[Z] = \begin{bmatrix} \langle t_1, L(g_1(z')) \rangle & \langle t_1, L(g_2(z')) \rangle & \dots \\ \langle t_2, L(g_1(z')) \rangle & \dots & \dots \\ \vdots & & \\ \langle t_N, L(g_1(z')) \rangle & \dots & \dots \end{bmatrix} , \quad (9)$$

$$\text{and } [V] = \begin{bmatrix} \langle t_1, E_z^1(z) \rangle \\ \vdots \\ \langle t_N, E_z^1(z) \rangle \end{bmatrix} \quad (10)$$

There are many possible choices for expansion functions and testing functions. Some combinations may produce faster convergence of the solution (require fewer functions for a given accuracy). Hence, smaller matrices are required, resulting in a savings of computer core. Other combinations may provide simpler computations of matrix elements, thus reducing computer run time. The most advantageous combination is currently under debate. Investigation of this important question is of paramount interest.

## 1.2 ELEMENTS OF A GENERAL-PURPOSE PROGRAM

The advantage of a general-purpose program is that extensive reprogramming is unnecessary whenever a new problem is addressed. Also, special-purpose input algorithms can be used to automate the problem specification, producing a highly user-oriented engineering tool. The user, however, must be cognizant of the program limitations set by the approximations inherent in the method of solution. Experience gained from exercising the program and sound engineering judgment are the keys to specifying the proper input data and interpreting the results.

Ideally, the input algorithms of a user-oriented general-purpose program will automatically divide each wire of the antenna structure into equal segments. (Equal segmentation has no special advantage except for ease in automation.) The user need only supply a description of the antenna structure in terms of the conductor radius, the end points of each wire, and the number of segments on each wire. Other parameters such as source location, magnitude, and frequency are also specified by the user. In each case, the parameters must be selected with good engineering judgment in order to produce worthwhile results.

A general-purpose program must of course possess the capability to deal with structures having multiple wire junctions. Some procedure must be implemented to extend the matrix solution for the case of multiple wire junctions. Although the precise boundary conditions applicable near the junctions are subject to debate,<sup>3</sup> it is generally agreed that the currents at junctions in thin-wire structures should obey Kirchhoff's current law. Hence, it becomes a bookkeeping job, preferably carried on by the computer, to keep track of junction locations and enforce the appropriate conditions on the currents.

Another important consideration is the selection of an appropriate source model. Fortunately, satisfactory results are obtained for a large number of problems by using the simplest source model, the delta gap. Occasionally a problem is encountered (for example, sources and junctions occur in close proximity) which may require a more elaborate source model such as the bicone source<sup>4</sup> or the magnetic frill.<sup>5</sup> Selection of the source is based on the user's experience.

### 1.3 COMPUTER CODES AT NELC

A number of computer programs using the approach outlined above have been acquired and exercised by the Radio Technology Division, Code 2100, at NELC. A list of these programs with their major attributes is given in table 1. Each is a general-purpose program. However, some are more user-oriented than others.

TABLE 1. THIN-WIRE COMPUTER CODES.

	<u>Frequency Domain</u>
AMP	(MB Associates) Sinusoidal Interpolation Point Matching Delta Gap Source Model
SYRACUSE	(Harrington, Kuo, Sraït, Syracuse University) Piecewise Linear Expansion Function Galerkin Technique Delta Gap Source Model
OSU	(J. Richmond, Ohio State University) Piecewise Sinusoidal Expansion Function Galerkin Technique Delta Gap Source Model
WHHP	(NELC) Piecewise Sinusoidal Expansion Function Point Matching Delta Gap Source Model
	<u>Time Domain</u>
TWTD	(Lawrence Livermore Laboratory) Quadratic Interpolation Point Matching Delta Gap Source Model

#### 1.3.1 AMP

The AMP program was developed under a tri-services contract by MB Associates.<sup>6,7,8</sup> This program uses a three-term current expansion<sup>9</sup> (which involves a constant, sine, and cosine term on each of the structure segments) with point matching and delta gap source model. AMP is a well written, very user-oriented general-purpose program. The input routines provide a useful and efficient means of specifying the geometry and electromagnetic environment for an antenna problem, which is the chief advantage of AMP. In addition to the original geometry routines, the capability to generate circular arc and helical wire structures has been added. Also added is the capability to compute the near magnetic fields.

Another unique feature incorporated into AMP is the option of choosing an alternative to the delta gap source model. The magnetic frill source model<sup>5</sup> may be specified for problems involving sources complicated by the proximity of junctions and other conductors.

### 1.3.2 SYRACUSE

The SYRACUSE program is a general-purpose program written by Kuo and Strait<sup>10</sup> using Harrington's approach of piecewise linear expansion functions with Galerkin's technique. Galerkin's technique is the method of moments approach in which the basis functions and testing functions are identical. Comparisons of this program to AMP indicate that the solutions converge faster (fewer expansion functions required for a given accuracy) with Galerkin's technique. The program employs a method of overlapping wires at junctions which enforces Kirchhoff's law. Although the source model is confused by the use of piecewise linear expansion functions, it is essentially a delta gap source.

To improve the utility of the SYRACUSE program, a data input package has been added to the original program. The user supplies the coordinates of wire end points, wire radii, wire connection data, and antenna environment parameters (excitation, frequency, etc). The input routines automatically segment the wires into equal segments and generate the overlaps at junctions. This represents a considerable improvement in the method of data input since it streamlines the problem definition.

### 1.3.3 OSU

The OSU program employs the piecewise sinusoidal reaction technique developed by J. Richmond.<sup>11</sup> The program utilizes piecewise sinusoidal expansion functions. The reaction technique is essentially the same as Harrington's method of moments with Galerkin's technique. The program also makes use of a wire overlap scheme at junctions (similar to that of the SYRACUSE program) and employs the delta gap source model. OSU offers faster convergence than AMP, again because of Galerkin's technique and the ability to evaluate some of the integrals in closed form (an advantage of the sinusoidal expansion functions). Presently, however, OSU is limited in capability since it is not user oriented (as is AMP) and can only treat structures with equal-radius wires. Effort is continuing to improve its capabilities.

### 1.3.4 WHIP

The WHIP (Whip Antenna Program) program was developed by J. W. Rockway and P. M. Hansen of Naval Electronics Laboratory Center.<sup>12</sup> WHIP is very limited in scope. It addresses only vertical whip antennas on an infinite, perfectly conducting ground plane. The program was written primarily to determine the near-field structure of Navy whip antennas. The program uses piecewise sinusoidal expansion functions with point matching and a delta gap source model.

### 1.3.5 TWTD

The TWTD (Thin Wire Time Domain) program is a product of the Lawrence Livermore Laboratory.<sup>13,14</sup> The program solves an electric field integral equation in time using the method of moments with subsectional collocation (quadratic interpolation with point matching). The source may be either a time-dependent incident field or a time-dependent version of the delta gap source model, depending on the user's choice. The program solves for the time-dependent induced currents which are used to find the time-dependent radiated or scattered fields. A discrete Fourier transform is used to determine the input impedance characteristics.

Input routines similar to those used in MBA have been added to TWTD to produce a highly flexible, user-oriented package. Also added is a plotting capability for easy display of time and frequency response characteristics of an antenna.

Presently, TWTD has the ability to treat resistive-loaded structures only. It is, of course, highly desirable to extend this capability to include reactive type loads.

## 1.4 PROGRAM LIMITATIONS

The solution to an antenna problem generated by any of the thin-wire programs is at best an approximation.<sup>15,16</sup> Nonetheless, highly accurate answers can be obtained by careful modeling of the antenna structure — by proper choice of segmentation and other relevant parameters. The accuracy of calculated antenna characteristics depends on how well the calculated current distribution conforms to the real case and hence on how well the antenna is modeled.

In general, for accurate results, the nearer to the antenna structure that calculated antenna characteristics are desired, the more accurately known must be the current. For example, it is well known that the assumption of a sinusoidal current distribution on a simple resonant dipole is sufficient to accurately determine the far fields. However, this approximation incorrectly predicts the input impedance.<sup>17</sup> Hence, higher resolution of the calculated currents is required for accurate determination of the impedance and near fields. The higher resolution is obtained by finer segmentation within the limits of the thin-wire approximation (segment length must be large with respect to wire radius).

The calculations of impedance and near fields often appear highly sensitive to the modeling of regions about feed points, wire junctions, and radius changes along the wires. The closer together these critical regions occur, the greater their influence on the results. The worst case occurs when junctions and large-radius changes are both in close proximity to feed point. In such cases, finer segmentation or more elaborate source models may be required.

## 1.5 CONFIDENCE FACTORS

Reliable, accurate results are obtained when the engineer has accumulated sufficient experience from frequent exercise of the program to recognize these problem areas. He must not only be aware of potential difficulties when initially setting up the program, but also when interpreting the results. Consequently, for each general-purpose program, the uninitiated user must run through a number of elementary problems, comparing the results to

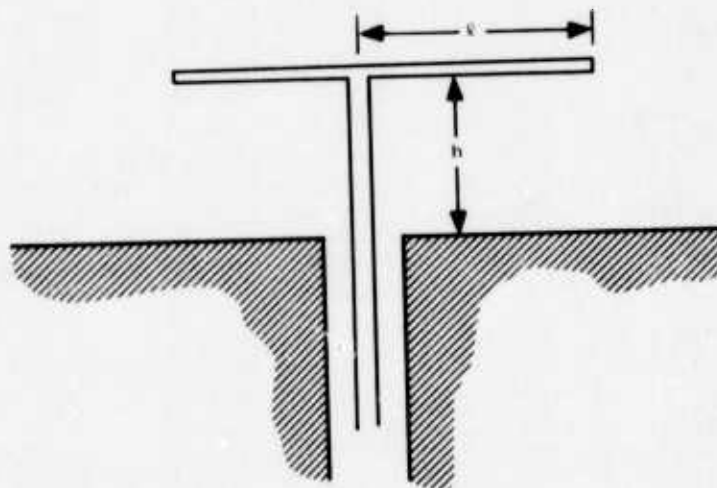
real world measurements, until he has the confidence to attempt new problems for which the answers are as yet unknown. Even then, the yardstick is always empirical data.

Development of this confidence factor entails modeling of a number of simple antenna structures found in standard antenna texts.<sup>18</sup> The approach is to progress from the simple case to the more complex. A natural first choice is dipoles in free space or monopoles on a ground plane, followed by inverted L antennas and T antennas, etc. For each antenna type, a number of problems involving different wire radii and lengths are selected, and the segmentation is varied until the solution converges. Comparison with measured data then provides the insight required for effective application of the computer program to problems for which empirical data may be sketchy or unavailable.

An example of the type of problem used in this initial program validation is the T antenna<sup>19</sup> shown in Table 2. Also shown are the "best" results using the various general-purpose programs along with empirical data.<sup>19</sup> This problem is presented as an example because it represents a significant step in the validation of the TWTB program. Figure 2 shows the time response of the feed point current to a Gaussian pulse, the Fourier transform of which is the input impedance given in Figures 3 and 4.

Another noteworthy problem is the 35-foot twin whip pictured in Figure 5. This antenna is similar to the standard 35-foot twin whip in common use throughout the Fleet. This problem is significant since the feed point region is complicated by the proximity of three junctions and two changes in radius. A comparison of the measured and calculated values of input impedance is given in Table 3. The measurements were made on the NELC ground plane. No values from the PSRT program are available, since in its present form it lacks the capability to account for differences of radii within the same structure.

TABLE 2. COMPARISON OF T-ANTENNA IMPEDANCE COMPUTATIONS WITH THE MEASURED VALUES OF PARSAD.<sup>19</sup>



$$\frac{2\pi h}{\lambda} (h + l) = \frac{\pi}{2}$$

Radius of wire =  $0.004/\lambda$

	$\frac{2\pi h}{\lambda} = 0.2$	$\frac{2\pi h}{\lambda} = 0.5$
Measured <sup>19</sup>	$2.6 + j9.0$	$11 + j36$
AMP	$1.7 + j10.3$	$11 + j36$
SYRACUSE	$1.78 + j9.18$	$11.1 + j34.3$
PSRT*	$1.7 + j3.8$	$11.4 + j31.9$
TWTD		$11 + j34$

\*Answer limited by array sizes

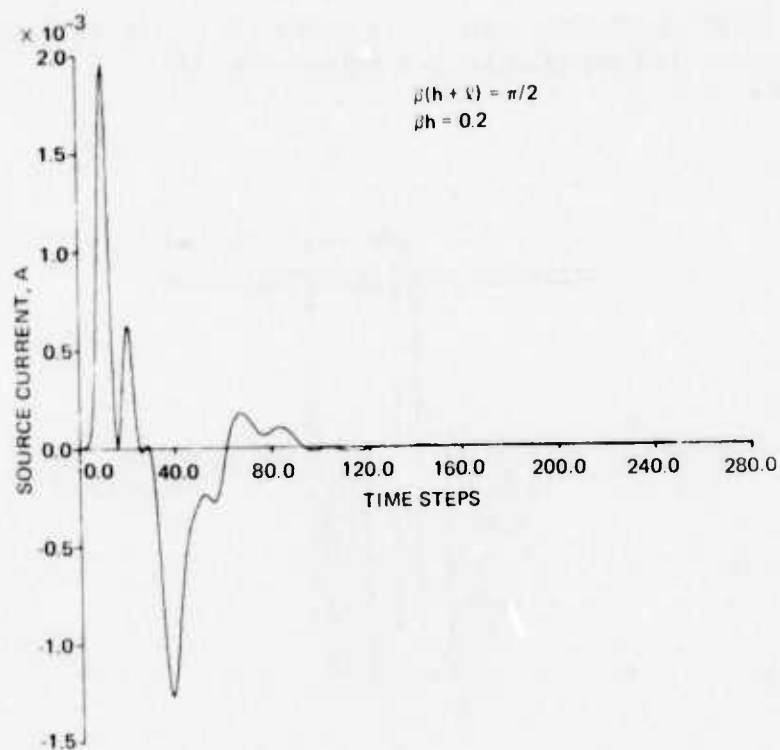


Figure 2. T-antenna time response to a Gaussian pulse.

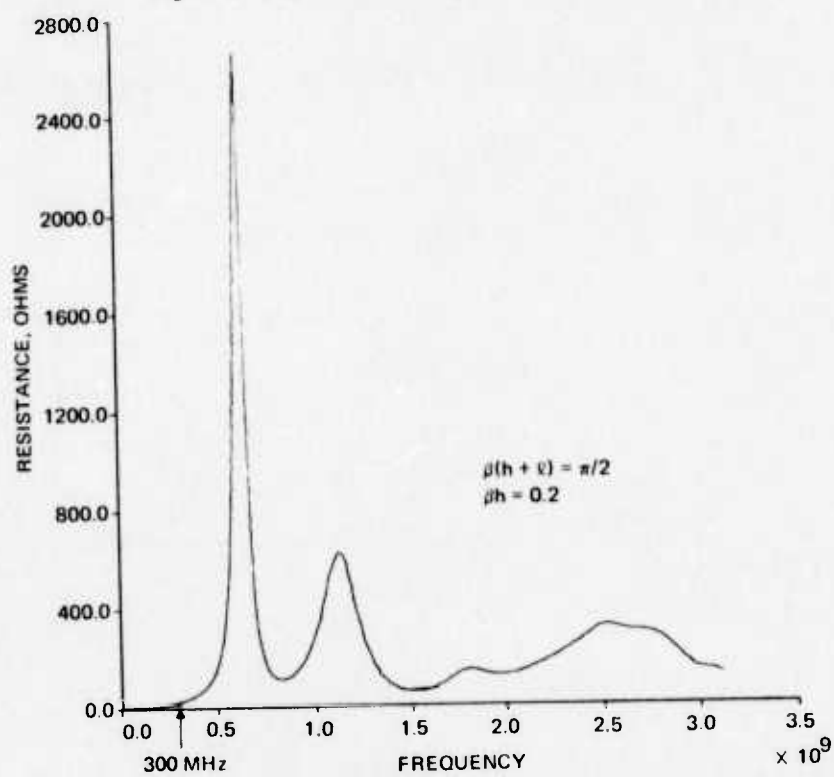


Figure 3. T-antenna frequency response – real component of input impedance.

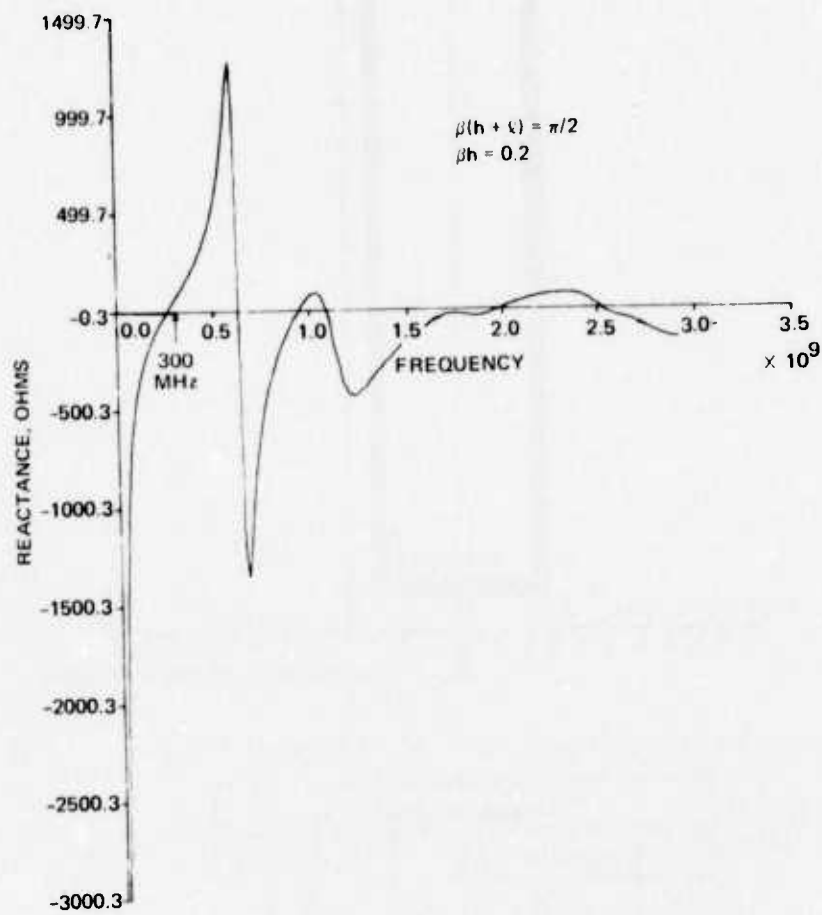
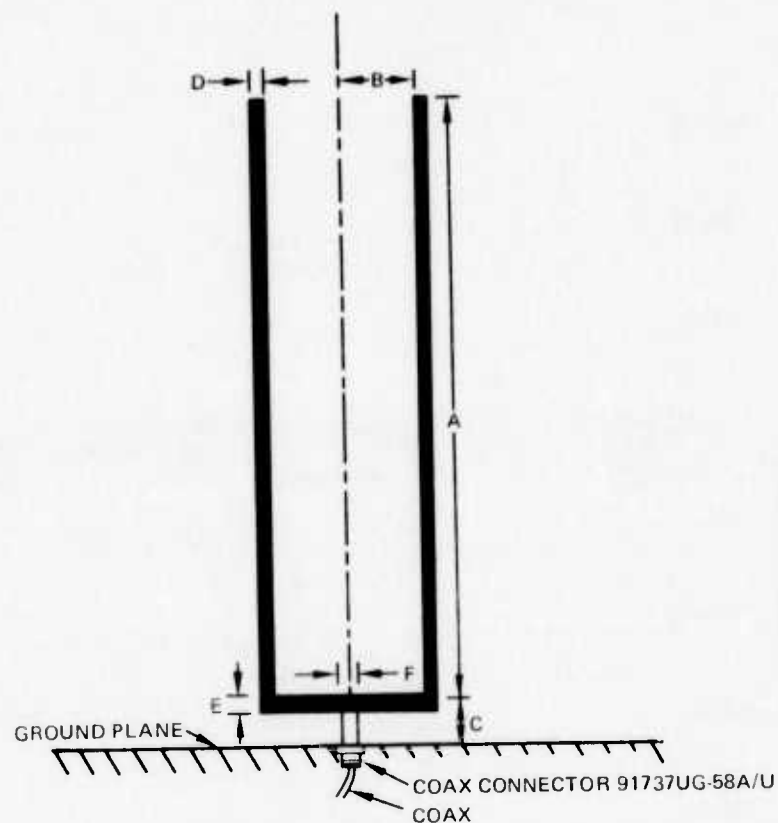


Figure 4. T-antenna frequency response — reactive component of input impedance.



DIMENSIONS, IN			
	LENGTH		DIAMETER
A	423.0	D	4.51
B	59.25	E	6.22
C	22.5	F	6.32

Figure 5. 35-foot twin whip over ground plane, dimensions.

TABLE 3. COMPARISON OF MEASUREMENTS AND COMPUTATIONS OF A 35-FOOT TWIN WHIP.

	4 MHz	6 MHz	8 MHz
Measurement	$9.0 - j101.5$	$29.0 - j9.0$	$80.0 + j67.5$
AMP	$9.89 - j70.0$	$34.1 + j18.4$	$114.0 + j86.56$
SYRACUSE	$8.45 - j77.5$	$29.8 + j2.01$	$101.4 + j57.8$

## 2.0 SPECIFIC APPLICATIONS

After developing sufficient confidence in the accurate application of the general-purpose thin-wire modeling programs, it becomes possible to utilize the programs as worthwhile engineering tools. The remainder of this report is concerned with the application of these engineering tools to support the antenna analysis work in the Radio Technology Division of NELC. Four examples are discussed in some detail. These four examples are concerned with the following projects:

1. HF Antenna System Design for Patrol Hydrofoil (Missile) (PHM)
2. MLA-1 Miniloop Antenna: A Technical Evaluation
3. AN/PRC-104 Antenna Improvement Study
4. Evaluation of Multiturn Loop Antenna

In each example the specific project is outlined and the antenna analysis problems of particular interest are described. Of particular interest are those technical problems for which the general-purpose thin-wire modeling programs were utilized. The actual utilization of the numerical modeling programs is described in some detail while other aspects of the engineering problem are discussed only as required to lend support. The primary objective of these examples is to demonstrate both where and how the general-purpose numerical modeling programs can be used as useful engineering tools. Again, whenever possible, in order to build further confidence in the numerical modeling capability, the analysis is compared to empirical data. Building of this confidence factor is always a continuing process.

In almost all the work described, the principal general-purpose program utilized is the AMP program. In many applications, it was necessary to modify the existing AMP program, and these modifications are noted. Some of the associated subroutines are listed in the appendices for the convenience of readers who make use of the AMP program.

### 2.1 HF ANTENNA SYSTEM DESIGN FOR THE PATROL HYDROFOIL<sup>20</sup>

The Patrol Hydrofoil, Missile (PHM), is a high-speed patrol craft planned for use by NATO forces. Two prototype vessels are being designed and built under Navy contract by the Boeing Aerospace Company. The small size of the PHM — length 40 meters — coupled with the requirement for a rather extensive communication capability for this size ship, in addition to weapon requirements, poses difficult antenna placement problems. This is especially true at hf where antenna spacings, in terms of wavelength, are small by necessity.

NELC was tasked by NAVSHIPS, PMS-303.6, to perform an hf antenna system design study in conjunction with the overall communications design effort being pursued by Boeing. Requirements for the hf (2–30 MHz) subsystem on the PHM specified two 1-kW transceive circuits capable of simultaneous operation and capable of providing gapless 556-kilometer coverage. Limited topside space available for antennas precludes the use of broadband antennas with multicouplers. Thus, the antenna system devised consists of two separate antenna structures: (1) a whip antenna on the port side, just aft of the pilot house at the 01 level, and (2) a three-wire, bent-fan antenna, strung from the mast aft and fed at deck level (see Figure 6). A second whip was installed parallel and starboard of the first whip to provide a backup receive circuit.



Figure 6. Scale model of patrol hydrofoil (missile) (PHM).

One of the primary restrictions on the hf communication system is that the two candidate hf antennas must be so arranged that they meet the HERO (Hazards of Electromagnetic Radiation to Ordnance) requirements for the PHM weapons: the Harpoon missile launcher aft and the OTO MELARA gun forward. The Naval Ordnance Systems Command has established classification of susceptibility pertinent to HERO.<sup>21</sup> Susceptibility refers to the actual induction of measurable rf energy into the electroexplosive devices (EEDs) in an ordnance system. The degree of susceptibility depends upon the amount of induced energy, the characteristics of the EED, and the electric field environment.

For this project it was necessary to predict the electric field intensity at both of the PHM weapon sites. Thin-wire modeling computer calculations were used to predict the maximum expected peak electric fields for the antenna-to-weapon spacings chosen. Discussions of these results appear in the next two sections (2.1.1 and 2.1.2).

Another important problem is that of strong coupling between hf communications systems due to the close proximity of the antennas. This problem arises on the PHM because of the limited available topside space and a requirement for simultaneous operation of two separate hf transmit systems.

In the PHM case, the problem of coupling has been solved by using a fan as one transmit antenna and a whip as the other. Two whips placed at the separation distance of the fan and whip do not provide sufficient isolation. On the other hand, the fan-whip combination has the required isolation.

In this case, isolation data were determined empirically. However, it is possible to analytically compute isolation. As a demonstration of this capability, the isolation between two whips on a ground plane has been computed. Section 2.1.3 contains a discussion of the analytical approach and a comparison to empirical data.

### 2.1.1 WHIP NEAR FIELDS

The transmitting whip is the primary contributor to the electric field intensity in the vicinity of the OTO MELARA guns. Electric near-field calculations were made with the NELC Whip Antenna program for perfectly conducting whip antennas of lengths 5.33 meters (17.5 feet) and 10.67 meters (35 feet). At one time both lengths were considered as candidate antennas. Analytically, the calculations were made for the antennas on an infinite, perfectly conducting ground plane.

Figure 7 defines Case 1 as the 10.67-meter whip and Case 2 as the 5.33-meter whip. A coordinate system with respect to the whips is also defined. Figures 8 and 9 show the computed peak electric near field at varying heights above the ground plane and at varying distances from the candidate whip antenna. The peak field is not directly related to the sum of the squares and must be calculated by the method described in Reference 22. For further information concerning these calculations, also see Reference 12.

The efficiencies referenced in these figures are for the URA/38 coupler attached to the whip antennas. The losses associated with the whip antennas themselves are negligible compared with the losses of the coupler.

The maximum electric near field at a fixed distance away from an antenna occurs at the lowest operating frequency. In Figure 6 the minimum distance to the OTO MELARA gun is approximately 7 meters. Thus, at the lowest operating frequency of 2 MHz the peak

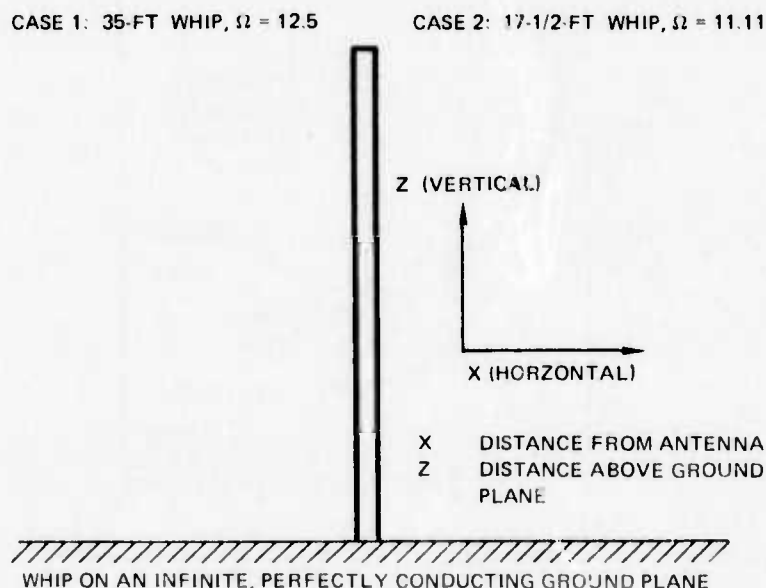


Figure 7. Whip on infinite, perfectly conducting ground plane.

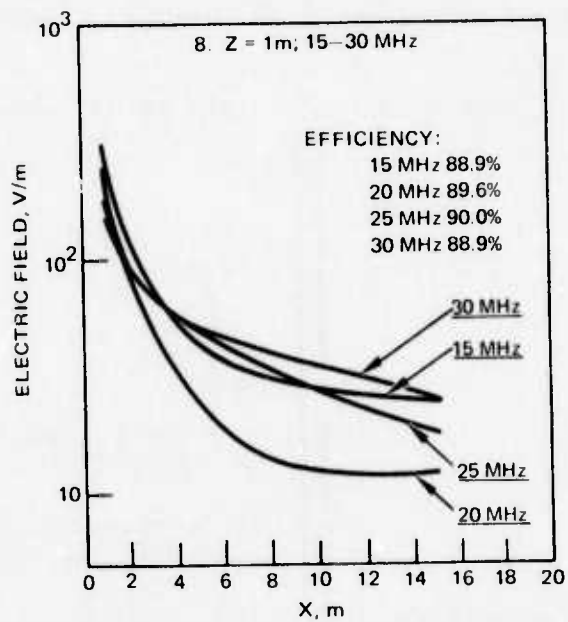
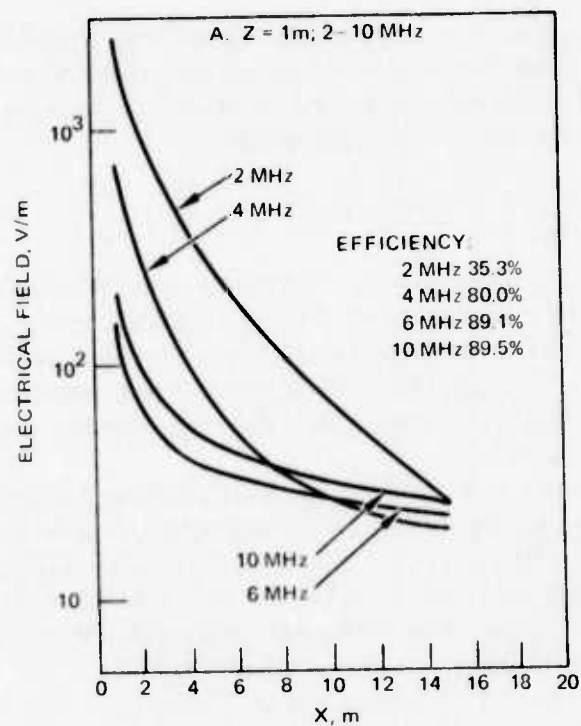


Figure 8. Peak electric field at various frequencies (derated for coupler losses; 1.0 kW into coupler); case 1; 1 kW into coupler.

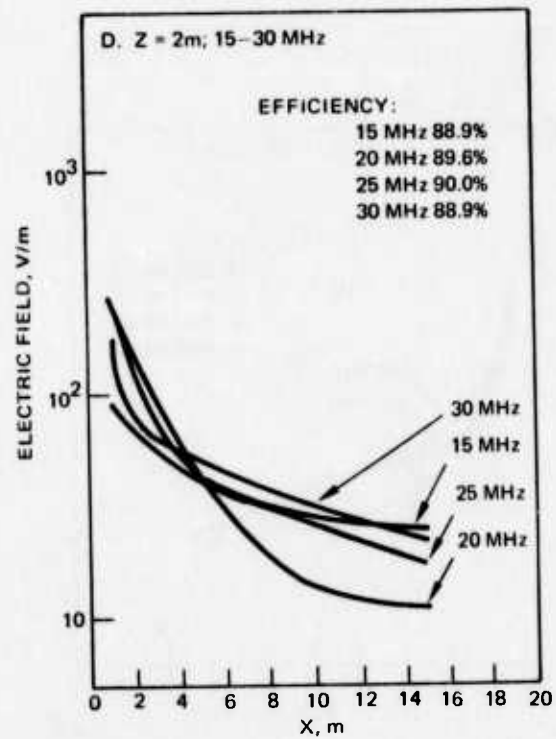
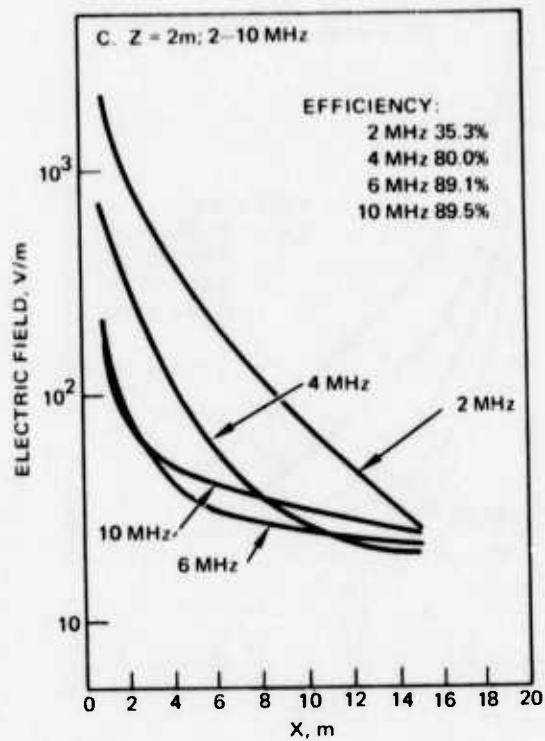


Figure 8. (Continued)

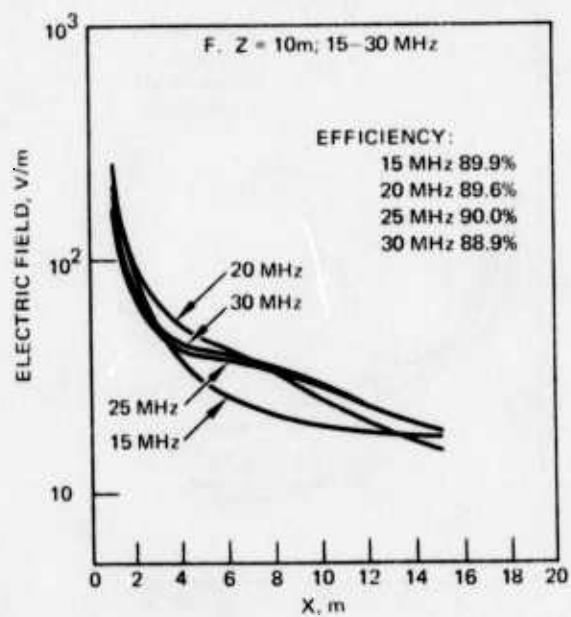
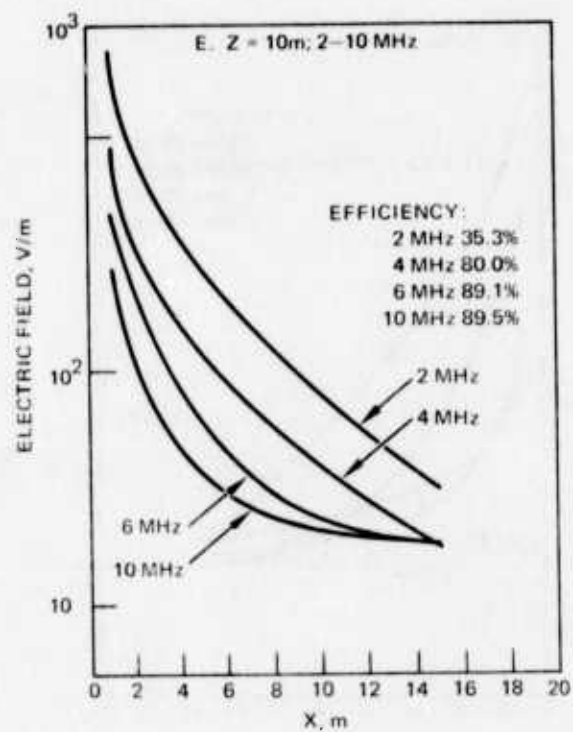


Figure 8. (Continued)

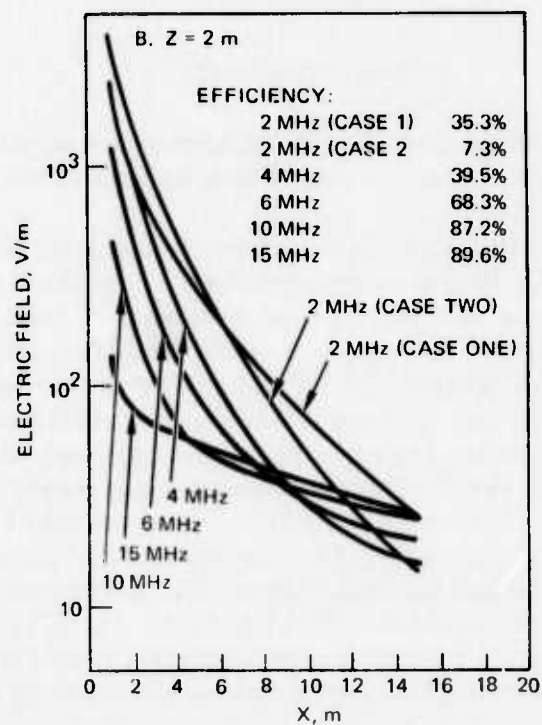
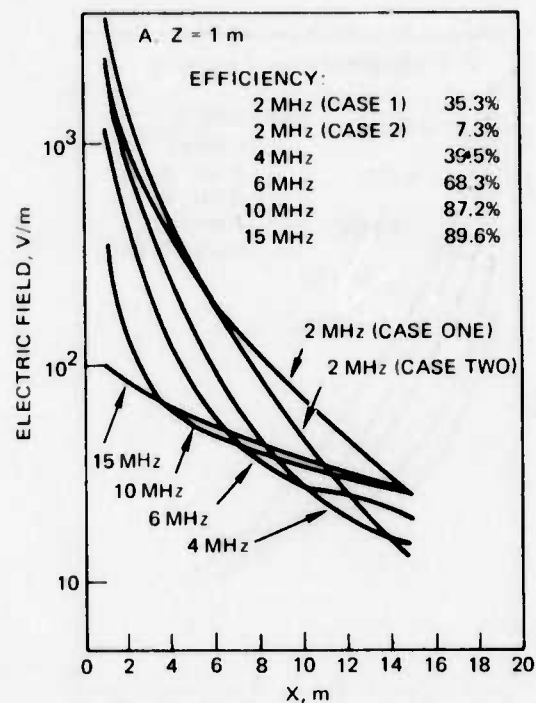


Figure 9. Peak electric field, 2 - 15 MHz (derated for coupler losses: 1.0 kW into coupler); case 2: 1 kW into coupler.

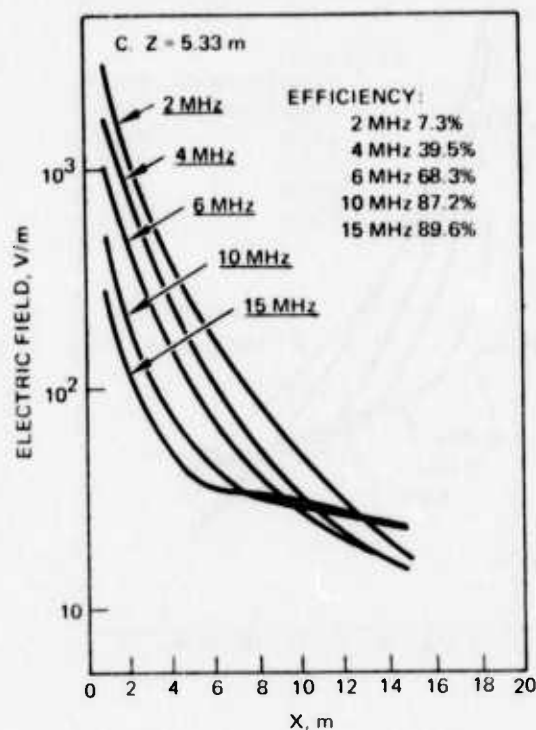


Figure 9. (Continued)

electric field at 1 meter above the deck and with an antenna-to-weapon spacing of 7 meters is 115 rms volts/meter for the 5.33-meter whip (Figure 9A) and 81 rms volts/meter for the 10.67-meter whip (Figure 8A).

These computed results for a whip on a perfect ground plane can be extrapolated to the whip on the PHM. In TR 1872 it is concluded that the near electric field is not a major function of the structured environment surrounding the whip.<sup>12</sup> Further, the whip on the PHM is situated 1.9 meters above the main deck. In Figure 10 the computations for an appropriate sleeve monopole are compared with the computed electric near fields of the 10.67-meter whip at 2 MHz. The sleeve monopole is fed 1.9 meters above ground and it extends 10.67 meters above its feed point. The computations are again made above a perfect ground. Near the antenna the electric near field of the sleeve monopole is somewhat less than the electric near field of the 10.67-meter whip. Thus, the computations of Figures 8 and 9 are representative of the actual electric near fields which would occur onboard the actual PHM.

It is of interest to compare the computations of several numerical modeling programs. Table 4 lists the computed results of the AMP, SYRACUSE, and NELC programs for the 10.67-meter whip at 2 MHz over a perfect ground plane. The near-field results are all within 5% of each other. It is encouraging that there is this agreement among the computer programs.

In conjunction with the analytical computations, near-field measurements for a whip over an extended ground plane were made with an E-field sensor, EFS-1, manufactured by Instruments for Industry, Inc. Figure 11 compares these measurements with the

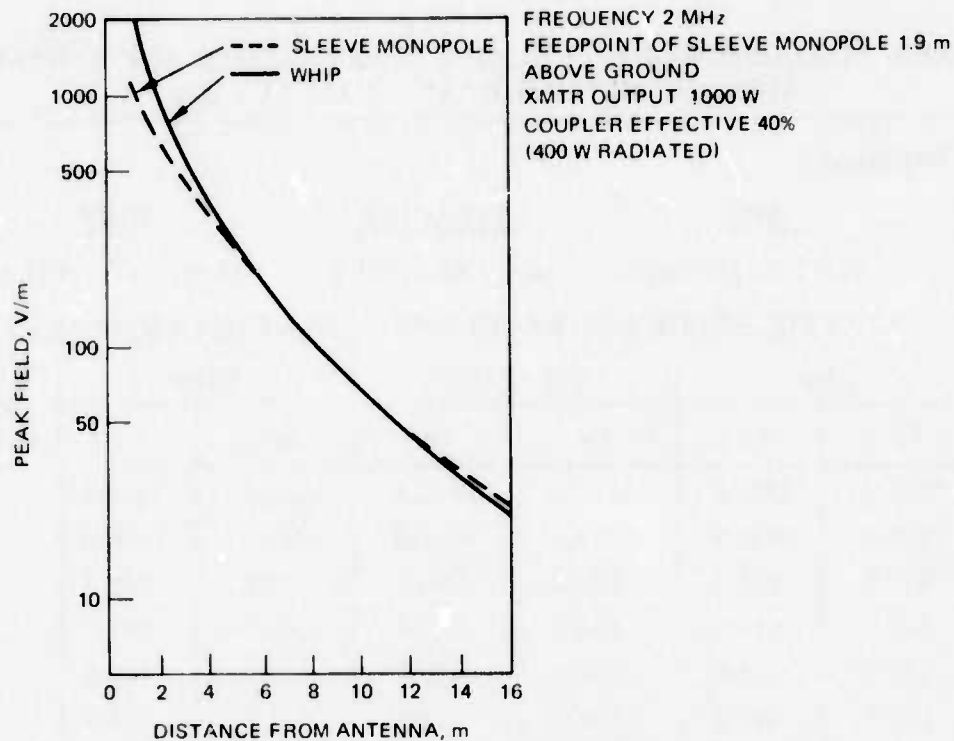


Figure 10. Comparison of calculated electric near field of whip and sleeve monopole.

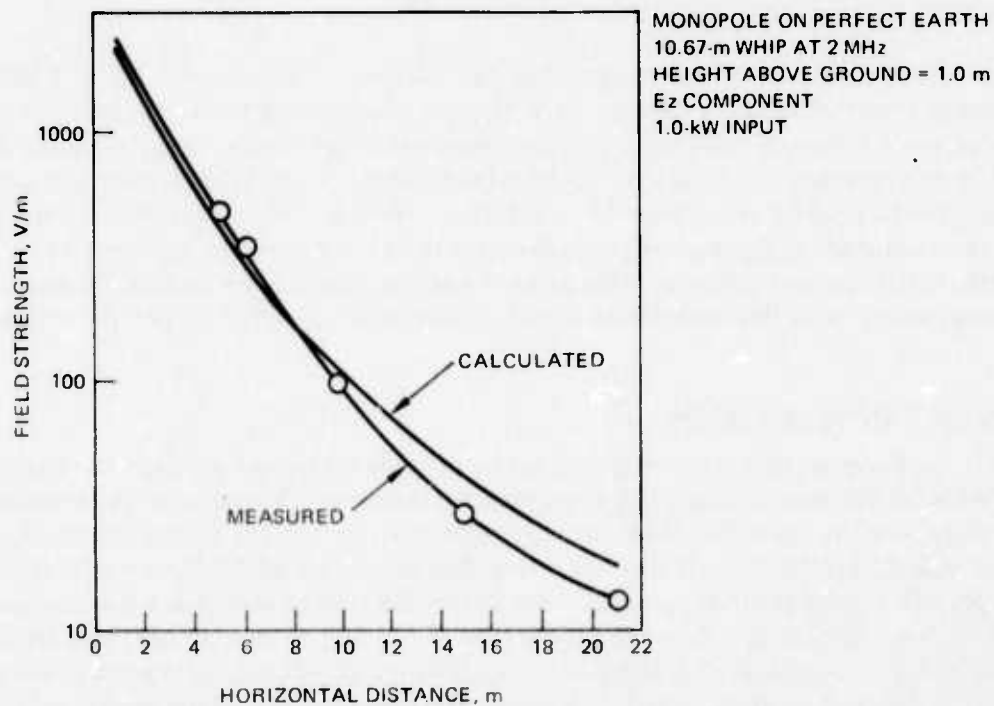


Figure 11. Comparison of measured and calculated peak electric near fields for case 1 at 2.0 MHz ( $z = 1.0$  meters).

TABLE 4. COMPARISON OF CALCULATED NEAR FIELDS OF AMP, SYRACUSE, AND WHIP 10.67-METER WHIP ANTENNAS AT 2 MHz.

Impedance:

$$\begin{array}{ccc} \text{AMP} & \text{SYRACUSE} & \text{WHIP} \\ Z = 2.0 - j571.95 & Z = 1.88 - j563.1 & Z = 1.782 - j552.4 \end{array}$$

NEAR FIELDS FOR 1000 WATTS INPUT - 1.0 METER ABOVE DECK

AMP		SYRACUSE		WHIP		Meters from Antenna
Ex	Ez	Ex	Ez	Ex	Ez	
3435.2	2406.5	3655.4	2612.4	3468.0	2368.0	1
1013.9	1404.9	1072.5	1467.8	1019.0	1400.0	2
450.0	875.1	472.4	906.2	452.8	873.3	3
248.1	589.8	256.9	606.4	247.9	587.2	4
153.2	418.0	157.8	428.1	153.0	415.5	5
101.9	307.2	104.6	313.5	101.7	304.3	6
29.2	110.8	29.6	112.3	28.9	106.8	10
9.2	42.2	9.3	42.6	9.1	40.7	15
3.2	19.6	3.3	19.7	3.2	19.5	21

computations of the NELC program for the case of the 10.67-meter whip at 2 MHz. The comparisons are made at 1 meter above the extended ground plane. As previously pointed out, the accuracy of any computation improves with the distance away from the antenna. For example, the computation of the far-field pattern is significantly more accurate than the computation of the impedance for any antenna structure. Thus, in Figure 11 the computational accuracy of  $E_z$  improves with distance away from the whip antenna. Thus, the increased discrepancy between measurement and calculation is attributable to measurement inaccuracy. With this consideration, the calculations compare well with the measurements.

## 2.1.2 FAN NEAR FIELDS

Because of the structural complexity of the fan antenna, calculation of the electric near fields for this antenna is a much more difficult problem. The radius of the linear elements comprising the fan differs from the supporting mast by a factor of more than 50. If elements of such different radii were directly connected, inaccurate calculations would result. In the case of a top-fed fan, this condition may exist. For such an antenna, a thin-wire computation would not be possible. However, in the case of this bottom-fed fan, the mast and fan are not electrically connected. A numerical computation of acceptable accuracy can be made.

A fairly complex model (125 segments) of the fan and its supporting mast was simulated with the AMP program. Limited electric near-field data at 2 MHz were computed at varying

distances. Again the maximum near field at a fixed distance away from an antenna occurs at the lowest operating frequency. Near-field measurements with the EFS-1 were made of a full-scale mock-up of this fan antenna and supporting mast. The mock-up was constructed on an extended ground plane. The results of these calculated and measured electric near fields are given in Table 5. (The Harpoon missile is situated 12 to 14 meters from the mast.)

### 2.1.3 ISOLATION

Consider the case of two 10.67-meter whips (standard 35-foot Navy whips) separated 7.6 meters on an extended ground plane. The isolation between these antennas can be computed by treating this coupling problem as a two-port network problem. This requires only one run of the AMP program for each frequency to determine the two-port network admittance parameters ( $Y_{11}$ ,  $Y_{12}$ ,  $Y_{21}$ , and  $Y_{22}$ ). Due to the symmetry of the problem,  $Y_{11} = Y_{22}$ . Also, since the network is bilateral,  $Y_{12} = Y_{21}$ .

Once the admittance parameters have been found, the input impedance and coupling can be determined for arbitrary loading conditions. Straightforward network analysis yields the following relationships for an arbitrary two-port system.

$$Z_{in} = \frac{Y_{22} + Y_L}{Y_{11} Y_{22} - Y_{12}^2 + Y_{11} Y_L} \quad (11)$$

and

$$\text{isolation} = \frac{P_2}{P_1} = \frac{R_e Y_L}{R_e Y_{in}} \left| \frac{Y_{12}}{Y_{22} + Y_L} \right|^2, \quad (12)$$

where  $Y_L$  is the arbitrary load admittance. For a complete discussion of this topic see Reference 23.

Equations (11) and (12) have been written into an interactive basic computer program called "Nonradiating Network Program." A listing of this program is given in Appendix A. The short-circuit admittance parameters and load admittance,  $Y_L$ , are input to the program. The program computes  $Z_{in}$  and the isolation in dB ( $10 \log P_2/P_1$ ).

Figure 12 shows the isolation in dB versus frequency for two sets of independent measurements. The computed isolation compares well with the empirical data.

TABLE 5. NEAR FIELDS OF FAN ANTENNA.

Frequency = 2.0 MHz

Coupler Losses = 5.1 dB

#### VERTICAL COMPONENT OF NEAR FIELD AT 1 METER ABOVE GROUND PLANE

Distance from Mast	Measured	Calculated
12.5 m	50 V/m	60.9 V/m
13.5 m	38 V/m	46.3 V/m
14.5 m	30 V/m	35.9 V/m

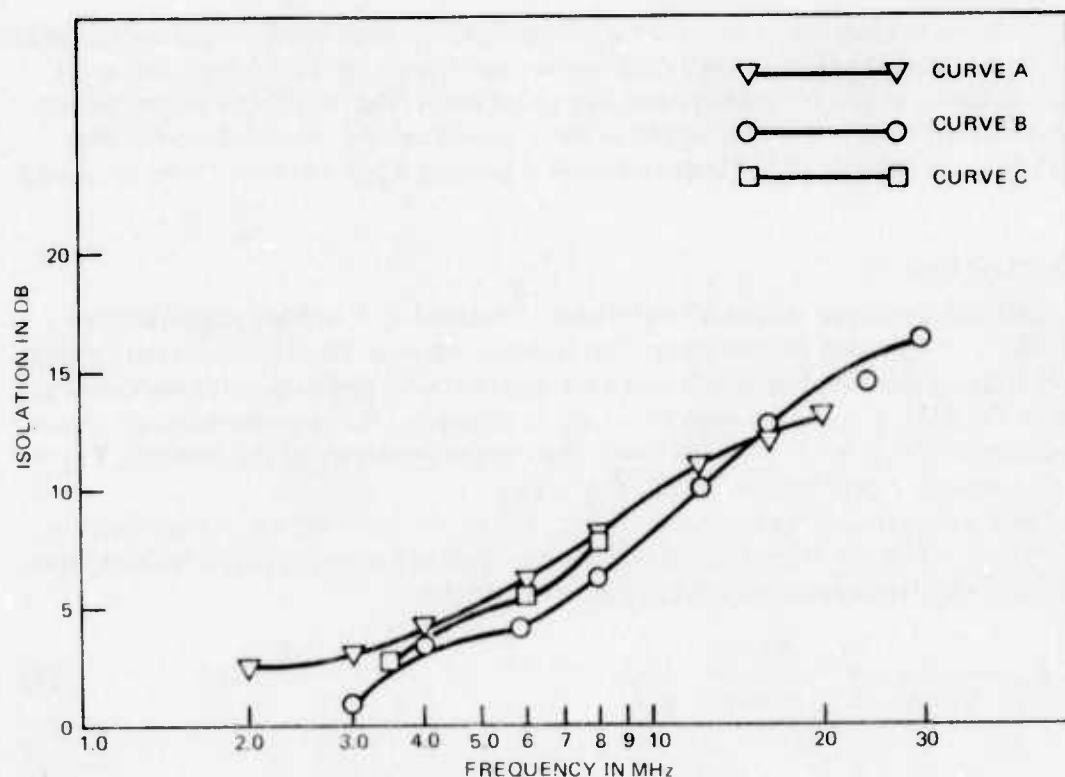


Figure 12. Isolation between two 10.67-meter whip antennas spaced 7.6 meters apart over a ground plane. Curve A is taken from measured data in NELC TR 138<sup>24</sup>. Isolation is based on power transfer from one whip to a second terminated in a conjugate match. Curve B is based on measured data taken on the NELC ground plane with both whips matched at each frequency using AN/URA-38 antenna couplers and corrected for coupler loss. Curve C is based on numerical modeling calculation.

## 2.2 MLA-1 MINILOOP ANTENNA: A TECHNICAL EVALUATION<sup>25</sup>

NELC was tasked by Naval Electronic Systems Command (NAVELEX) to technically evaluate the Antenna Research Associates, Inc., Miniloop antenna type MLA-1. The frequency range of this antenna is 1.8 – 14.5 MHz. Figure 13 shows the Miniloop installed.

Thin-wire modeling supported this evaluation in the following three areas: (1) determination of efficiency, (2) determination of near electric and magnetic fields, and (3) validation of the 1/48th scale model of the Miniloop for patterns. Discussions of these topics are contained in sections 2.2.1, 2.2.2, and 2.2.3, respectively.

In order to facilitate the modeling of the Miniloop antenna, an arc subroutine was added to the geometry package of AMP. This subroutine is called in a manner similar to subroutine WIRE from subroutine DATAGN. A listing of subroutine ARC is given in Appendix B along with a description of the appropriate geometry card. This description follows the format of the AMP User's Manual.<sup>7</sup>



Figure 13. MLA-1 Miniloop installed aboard USS BRADLEY (DE 1041).

### 2.2.1 EFFICIENCY DETERMINATION

An attempt was made to determine the absolute efficiency of the Miniloop antenna; that is, the ratio of the power actually radiated to the power fed to the antenna. The efficiency of any small (small in terms of wavelength) antenna can be expressed by:<sup>26</sup>

$$\eta = \frac{Q_{\text{measured}} \times R_a}{X_a} \times 100\% , \quad (13)$$

where  $R_a$  and  $X_a$  are the radiation resistance and the reactance of an ideal antenna (no losses) and  $Q_{\text{measured}}$  is the "Q" of the actual antenna derived from bandwidth measurements. In the case of the Miniloop,  $R_a$  and  $X_a$  were determined by using the AMP program. The Q was measured on the test antenna. These values were inserted into equation (13) to obtain efficiency. This ability of thin-wire modeling programs to model lossless antennas is valuable in determining the efficiency of any small antenna.

### 2.2.2 NEAR FIELDS

Because shipboard operations are carried out within fixed (small) distances from hf transmitting antennas, the Navy has a unique and longstanding operational problem:<sup>27</sup> the radiation from these antennas can be hazardous to personnel, ordnance, fuel, and electronic equipment due to the intensity of the fields in close proximity to the radiating element.

Near-field computations were made for both the electric and magnetic components of the Miniloop antenna. Special emphasis was placed on the magnetic field determination because theoretically the near magnetic field is greater for the MLA-1 antenna than for the other communication antennas presently installed on Navy ships. Also, recent developments<sup>28</sup> have placed greater emphasis on the radiation hazards of magnetic fields to personnel.

In order to make the magnetic field calculation, the AMP program was modified. The three subroutines NHFLD, GH, and HFK were added to the code. NHFLD is called from the main program in the same manner as NEFLD. The magnetic fields are calculated in amperes/meter. A listing of subroutines NHFLD, GH, and HFK is given in Appendix C. The magnetic fields thus computed compare well with the calculations reported in Reference 29.

The AMP program was used to make calculations of electric and magnetic fields at 2.0 MHz and a radiated power of 1 kW, the maximum power rating of the MLA-1 Miniloop antenna. Again, 2.0 MHz was chosen because it is close to the lower limit of the tuning range of the antenna where at a fixed distance the near-field strength is greatest.

Figure 14 presents selected computer-predicted near-field magnetic component data for a lossless loop antenna having the dimensions of the MLA-1 Miniloop when radiating 1 kW at 2.0 MHz. Figure 14A is a family of curves indicating magnetic field strength as a function of distance from the antenna in the plane of the loop for several elevations above the ground plane. Figure 14B is a family of curves indicating magnetic field strength, as a function of distance from the antenna, in the vertical plane normal to the plane of the loop and including the axial centerline of the loop.

Figure 15 presents selected computer-predicted data for the near-field electric component of a lossless loop antenna having the dimensions of the model MLA-1/E Miniloop,

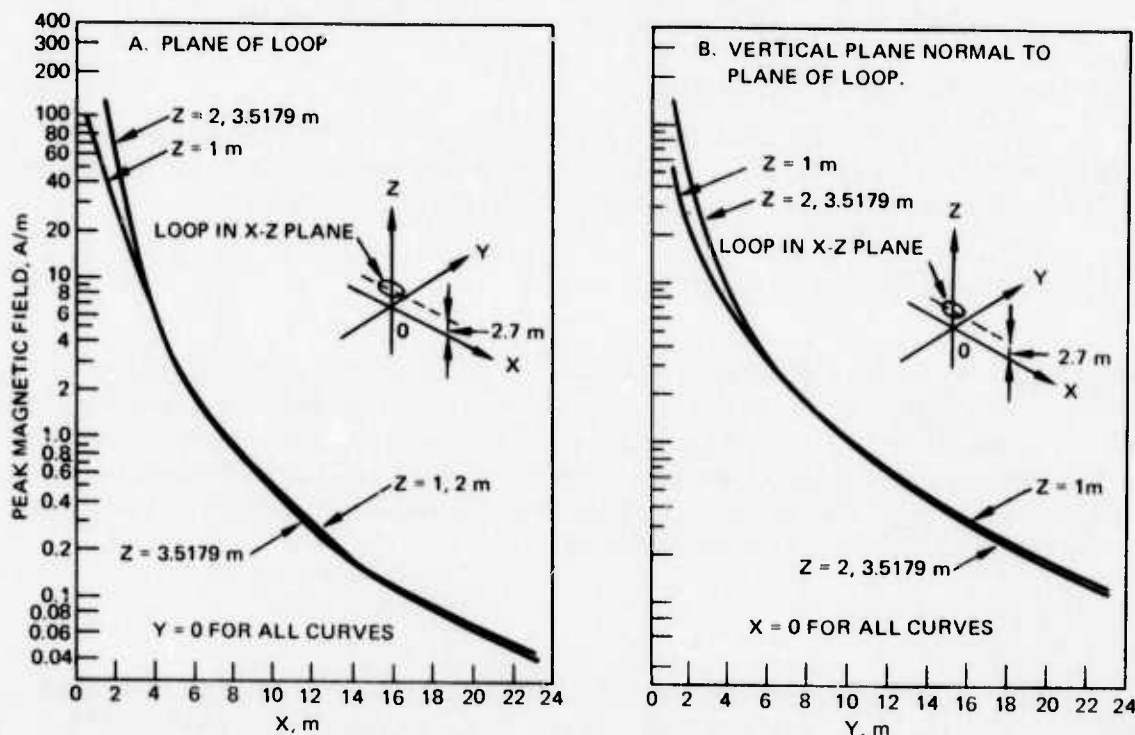


Figure 14. Computed values of peak magnetic field strength for the Miniloop antenna radiating 1 kW at 2 MHz.

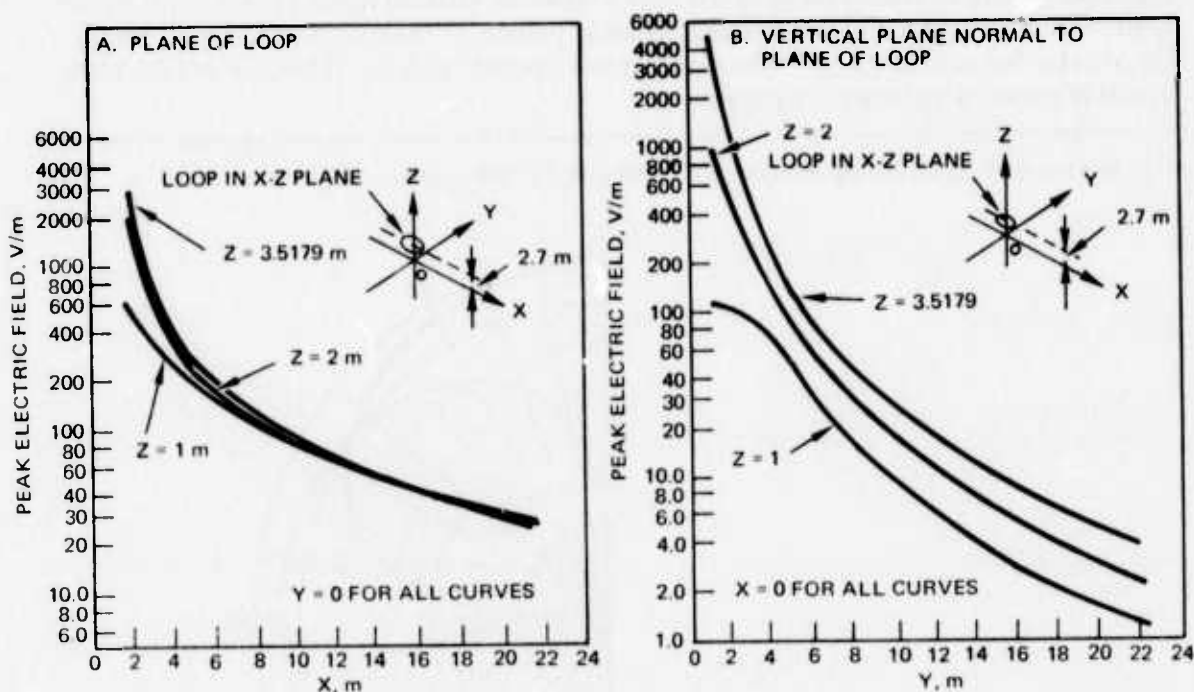


Figure 15. Computed values of peak electric field strength for the Miniloop radiating 1 kW at 2 MHz.

when radiating 1 kW at 2.0 MHz. Figure 15A is a family of curves indicating electric field strength as a function of distance from the antenna in the plane of the loop for several elevations above the ground plane. Figure 15B is a family of curves indicating electric field strength, as a function of distance from the antenna, in the vertical plane normal to the plane of the loop and including the axial centerline of the loop.

It must be remembered that the calculated curves are based on a lossless antenna radiating 1 kW. The Miniloop has very poor efficiency at the lowest frequencies where the near fields are greatest. For the real world Miniloop, the values shown must be decreased by the square root of the ratio of 1 kW to actual power radiated by the Miniloop.

### 2.2.3 PATTERN DATA

A 1/48th scale brass model of the Miniloop with supporting mast was built compatible with available brass ship models in inventory. However, the model was not an exact duplicate of the full-scale Miniloop. No attempt was made to duplicate the feed method used in the actual full-scale Miniloop. Rather, a one-turn, balanced, untuned, top-fed model was formed of semirigid copper coaxial line, 0.086 inch in diameter.

Since the model is not exact, it was questionable whether the model and full-scale antenna have the same radiation pattern. AMP was used to obtain analytically the inherent

radiation pattern of the actual Miniloop over a lossless, extended ground plane. This calculation was compared with the measured radiation pattern of the model Miniloop mounted on an extended ground plane.\* The two patterns compare exactly. Thus, the 1/48th scale model Miniloop is validated for patterns.

\* A comparison of the calculated and measured patterns at 2.0 MHz is given in Figure 16.

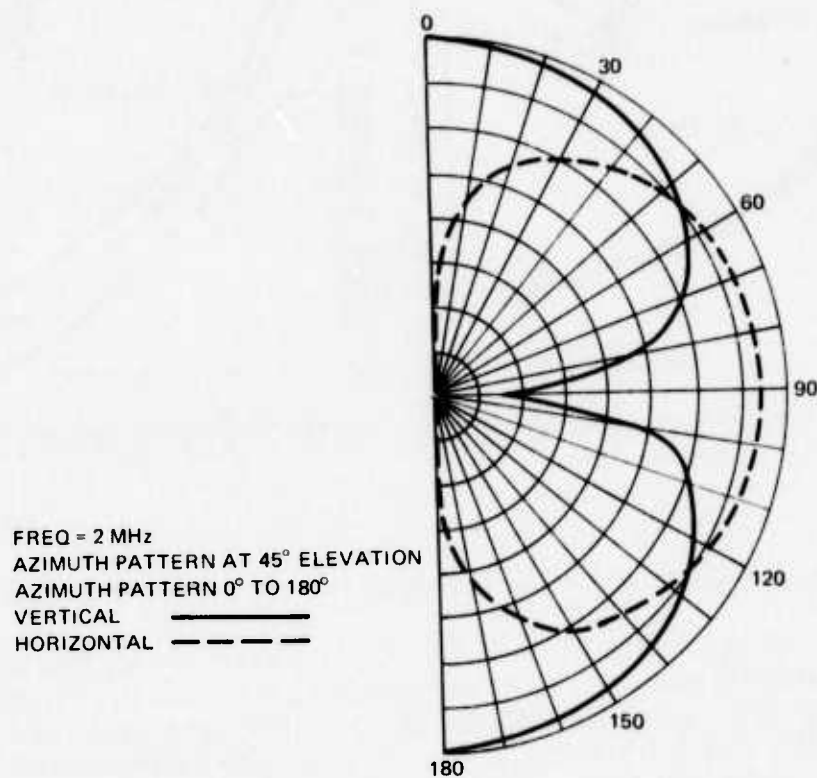


Figure 16. A comparison of the calculated and measured radiation patterns of the MLA-1 Miniloop antenna.

### 2.3 AN/PRC-104 ANTENNA IMPROVEMENT STUDY

NELC was tasked by NAVELEX to (1) determine if alternate antennas would improve the performance of the AN/PRC-104 above its present level when using an 8-foot whip and (2) demonstrate, if possible, how the existing system could be used to provide better performance in certain situations. The AN/PRC-104 is a Marine Corps man-pack, 2-30-MHz, 20-watt transceiver designed to use an 8-foot GFE whip antenna. The primary objective of this task was to improve the efficiency of the system at the low end of the band.

One of the most commonly suggested ways to improve the performance of a whip antenna is to use a series inductive load somewhere along the antenna. Short whip antennas have a "triangular" current distribution. Placing an inductor on the whip makes it electrically longer, and the current distribution is altered. If the proper inductance is placed at the tip of the whip, a constant current distribution results. One can determine the maximum change in radiation resistance caused by inductive loading by assuming an ideal situation, where all input power is radiated. Consider the two situations, one with the triangular distribution and one with a constant current distribution. In order for them to be equal radiators, the area under the current distribution curves must be equal. This implies the feed current of the constant distribution case is one half of the triangular feed current case. Thus, for equal power, the radiation resistance of the end-loaded whip is four times the unloaded whip resistance. This is the maximum improvement in radiation resistance attainable by loading.

The above discussion assumes an ideal inductor is used for loading. In reality, the inductor has loss and the question is whether the center load inductor actually improves the performance of the whip. The closer the inductor is placed to the tip of the whip, the larger the required inductance and thus the more loss resistance of the inductor.

C. W. Harrison<sup>30</sup> describes a monopole on a perfectly conducting, extended ground plane. The monopole is center loaded with an inductance of  $Q = 300$ . The monopole at 1 MHz has a height of 0.032 meter and a radius of 0.000123 meter. He then calculates the necessary inductance for resonance and determines the resulting efficiency. A similar calculation was made with the AMP program aided by the program in Appendix A. The program of Appendix A is very useful in determining the load necessary for resonance. The results are given in the table below.

TABLE 6. EFFICIENCIES OF INDUCTIVE-LOADED MONOPOLES.

	Harrison	AMP
$Z_{\text{no load}}$	$0.385 - j1350$	$0.49511 - j1573.9$
Efficiency		
Base loaded	7.88%	8.62%
Center loaded	19.85%	8.79%

The results of AMP differ considerably from Harrison's. However, the AMP results are independently supported by the analytical work of Reference 31. Obviously, some empirical work is needed in this area. However, due to sufficient confidence in numerical modeling, it was concluded for this study that fixed inductive loading along the antenna will provide little improvement above base inductive loading.

A similar problem was proposed to NELC by NAVSEC/NORDIV in Norfolk, Virginia. The question was whether the efficiency of a 35-foot whip at 1 MHz could be improved by inductive loading at the center of the whip. It was calculated that:

$$\eta_{\text{base loaded}} = 0.43\%$$

$$\eta_{\text{center loaded}} = 0.45\%$$

Again, in a quick response to the question, it could be stated that no improvement in efficiency was achievable by center loading.

## 2.4 EVALUATION OF MULTITURN LOOP ANTENNA

NELC evaluated, for shipboard application, the HF Multiturn Loop Antenna (MTL) developed by Ohio State University. The prototype model delivered to NELC is constructed from standard 2-inch copper tubing and fittings (Figure 17). It has the following characteristics:<sup>26</sup>

- Tuning range: 2 to 10 MHz
- Efficiency range: 1% to 30%
- Bandwidth: 3 kHz minimum (3 dB)
- Impedance over tuning range: Adjustable to exactly 50 ohms
- Input power: 1 kW
- Size of coil: (30.48 cm X 66.04 cm X 66.04 cm)
- Weight: 50 lb

The configuration of the MTL is a rectangular six-turn coil or helix with its axis and largest plane parallel to the ground plane. The separation of the lower coil side from the ground plane is only 4 inches.

One of the technical objectives of the NELC evaluation was to recommend a final design for both the transmitting and receiving functions. This section described how numerical modeling assisted in achieving that objective. Two aspects of this technical evaluation are discussed below; one concerns the arrangement of the tuning capacitor and the other concerns the orientation (horizontal vs vertical) of the MTL.

To the present, the study of hf antennas at NELC has been pursued almost entirely through the use of 1/48th scale brass models. The characteristics of the antenna were postulated on the basis of measured impedances and patterns. These are the effects. The numerical modeling approach computes the cause, the current distribution on the antenna. The ability to view the cause as well as the effects will lead to a better understanding of an antenna. Such is the case in the study of the MTL. This numerical modeling study has been pursued beyond the areas discussed here, providing useful insights into the antenna's characteristics. These insights will make a significant impact on the final helix design.

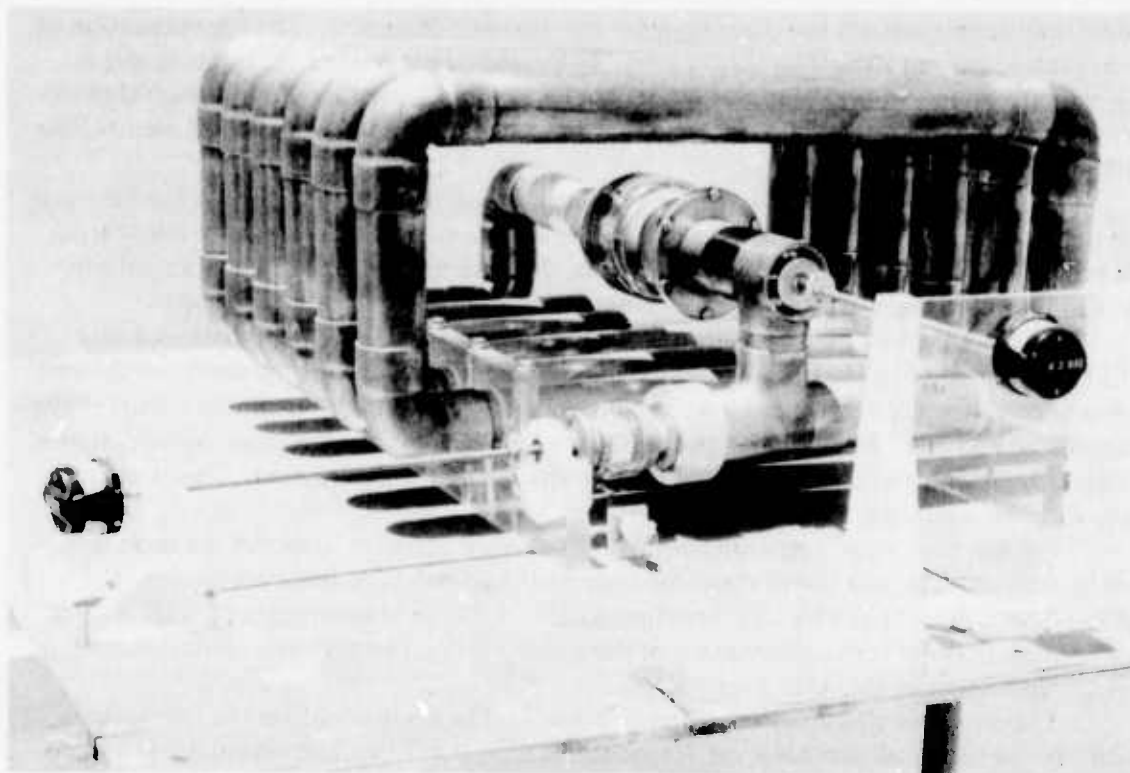


Figure 17. HF multiturn loop antenna of Ohio State University.

#### 2.4.1 BALANCED VS UNBALANCED OPERATION

One of the first aspects of the prototype model considered is the arrangement of the tuning capacitor. In its present configuration, the MTL tuning capacitor is across the entire coil. At a given resonant frequency, the two coil ends are high-impedance (low current) points. The single low-impedance (high current) point is at the center of the coil, midway between the ends. This is a "balanced" condition (the peak current occurs at the coil center with low current at coil ends).

A different configuration is made possible by the change from a "balanced" to an "unbalanced" antenna. For the unbalanced case, one end of the coil is grounded. The tuning capacitor is placed between the other coil end and ground. This arrangement has the electrical advantage of providing mechanical drive of the tuning capacitor at ground potential which helps to eliminate uncontrolled stray capacitance.

It was therefore suggested that the antenna be tuned in the unbalanced condition. The contractor, Ohio State University, responded that a greater tuning range is achieved with the tuning capacitor in parallel with the coil. In other words, the balanced condition offers a greater tuning range for a given change in capacitance. An attempt was made to verify this very important design question with the use of the thin-wire modeling tool. Several steps were required to arrive at the answer.

The first step is to frame the question in a manner such that thin-wire modeling is useful. Its applicability is limited by the thin-wire approximation. In the actual prototype

model, the conductors are too close together for thin-wire modeling. The approximation of no azimuthal current flow is no longer valid. In the present form, the MTL is basically a normal mode helix, so the computer model can be a larger normal mode helix such that the thin-wire approximation is valid. The MTL chosen for the computer model is 2 meters long with a helix radius of 0.239 meter.

The second step is to determine a suitable method of excitation so that the balanced and unbalanced conditions along the helix can be compared. In order to avoid introducing the problem of two different feed arrangements, the antenna can be treated as a scattering problem in which the excitation is an incident plane wave normal to the helix axis.

Figure 18 shows the configuration for the balanced case and the unbalanced case MTL. In the case of the balanced antenna, the current is maximum at the center of the coil at resonance. For the unbalanced antenna at resonance, the current maximum occurs at the ungrounded coil end. By observing the location of the current maximum as the capacitance is changed, the value of capacitance necessary for resonance is determined. This is easily done with the computer models.

For the third step, a new subroutine for the AMP program to model the helix structure is required. The new subroutine, subroutine HELIX, is called from subroutine DATAGN in a manner similar to subroutine WIRE. A listing of subroutine HELIX is given in Appendix D along with a description of the appropriate geometry card. This description follows the format of the AMP User's Manual.

The results of this study are given in Table 7. The results confirm the contractor's point. In the balanced case for a 2:1 frequency change, a 4:1 capacitance change is needed. In the unbalanced case, for a 2:1 frequency change, approximately an 8:1 capacitance change is needed.



Figure 18. Configurations of balanced and unbalanced MTLs.

TABLE 7. CAPACITANCE NECESSARY FOR RESONANCE FOR BALANCED AND UNBALANCED MTL ANTENNAS.

	Frequency	
	4 MHz	8 MHz
Balanced Antenna	800 pF	200 pF
Unbalanced Antenna	360 pF	50 pF

#### 2.4.2 HORIZONTAL VS VERTICAL CONFIGURATION

A second aspect of the design of the MTL concerns the orientation of the MTL with respect to ground. The axis of the present MTL is parallel to the ground plane. It has the structural configuration of Figure 19. A center support runs the length of the helix. Because of the coil's close proximity to ground, the imaging effect limits the inherent radiation of this MTL configuration. If the MTL is mounted with its axis vertical to the ground plane, as in Figure 21, the inherent radiating efficiency of the antenna should be improved since the conductors are further from the ground plane; that is, there is less cancellation of currents due to imaging.

To verify this important point, a comparison of the characteristics of the two configurations of the MTL was made using the AMP program. Figure 20 shows the impedance computed for the horizontal case and Figure 22 shows the impedance for the vertical case. Both antennas are base fed at the grounded end.

Since the prototype MTL is operated below the first natural resonance, the computer model comparison is also made below the first resonance for both configurations. The radiation resistance of the vertical helix is four to five times greater than the radiation resistance of the horizontal helix. The basic structure (dimensions) of both helix configurations is essentially the same, hence the loss resistance of both antennas is approximately the same. Thus, in a qualitative sense, the vertical configuration is a more efficient radiator.

### 3.0 CONCLUSIONS

The general-purpose thin-wire modeling programs provide a valuable engineering tool. They are a valuable asset in various phases of communication system development. As demonstrated in the case of the PHM study, the tool can assist in determining the effect of the antenna system on other systems. This is a valuable contribution to preliminary system planning. As in the case of the MTL and man-pack antenna projects, it can impact on the preliminary antenna design itself. As in the case of the Miniloop, test results can be evaluated and specifications prepared.

Typical problems that may be handled by the thin-wire modeling programs include the following:

- Determine current distribution on antenna systems.
- Determine impedances, both self and mutual, associated with antennas or arrays.
- Obtain near-field (electric and magnetic) components.
- Provide information on far-field patterns.
- Provide information on the RADHAZ of an antenna system.
- Provide information on the HERO consideration of an antenna system.
- Provide information on the efficiency of an antenna system.
- Examine the frequency characteristics of an antenna system.
- Examine the EMC situation for a complex of antennas and identify problem areas.
- Evaluate the impact of changes in antenna structures.

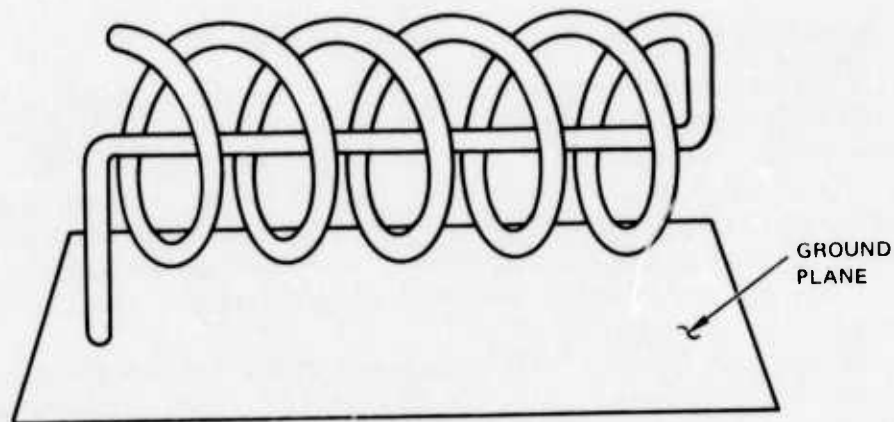


Figure 19. Horizontal helix with center support.

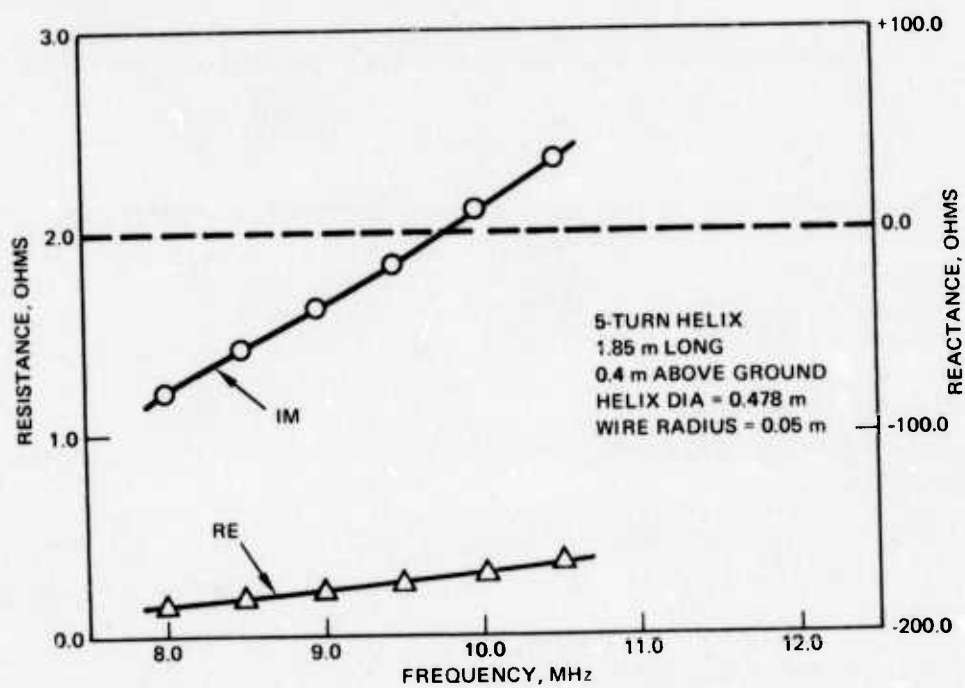


Figure 20. Computed resistance and reactance of horizontal helix with center support.

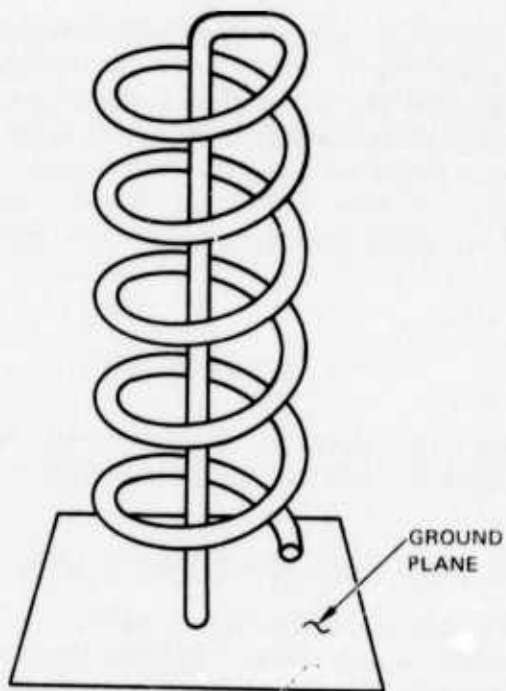


Figure 21. Vertical helix with center support.

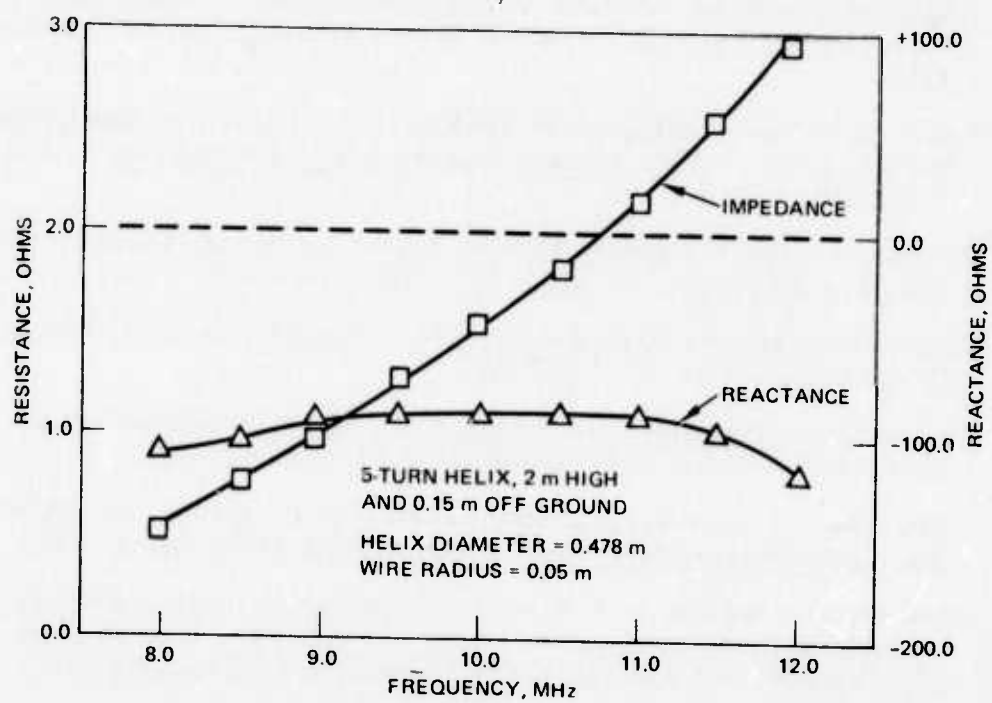


Figure 22. Computed resistance and reactance of vertical helix with center support.

In each case, effective use of numerical modeling as an engineering tool requires that the engineer be knowledgeable of the limitations of the numerical techniques. Such knowledge is acquired through frequent exercise of the computer programs and a continued study of the literature to keep abreast of developments as they occur. It should also be noted that the engineer is an integral part of the numerical analysis tool, since he plays the strategic role of properly posing the problems so that useful answers may be obtained as well as interpreting the computer output to extract an engineering solution.

### REFERENCES

- 1 Thiele, G. A., Wire Antennas, Chapter 2, a short course on "Computer Techniques for Electromagnetics and Antennas," University of Illinois, September 28 – October 1, 1970
- 2 Harrington, R. F., Field Computation by Moment Methods, The Macmillan Co., 1968
- 3 Logan, J. C., "A Comparison of Techniques for Treating Radiation and Scattering by Wire Configurations with Junctions," Syracuse University Technical Report TR-73-10 for the National Science Foundation Grant GK-4227, August 1973
- 4 Andersen, M. G., and Harris, F. B., Jr., "Analysis of Wire Antennas of Arbitrary Configurations by Precise Theoretical Numerical Techniques," Contract DAAB07-67-C-0631, Technical Report ECOM 0631-F, Granger Associates, Palo Alto, California, 1968
- 5 Tsai, L. L., "A Numerical Solution for the Near and Far Fields of an Annular Ring of Magnetic Current," IEEE Transactions on Antennas and Propagation, v. AP-20, no. 5, September 1972
- 6 MB Associates, Antenna Modeling Program, Engineering Manual, IS-R-72/10, office of Naval Research Contract No. N00014-72-C-0187, July 10, 1972
- 7 MB Associates, Antenna Modeling Program, User's Manual, IS-R-72/14, Office of Naval Research Contract No. N00014-72-C187
- 8 MB Associates, Antenna Modeling Program, Systems Manual, IS-R-72/10, Office of Naval Research Contract No. N00014-72-C-0187, April 10, 1973
- 9 Miller, E. K., and Deadrick, F. J., "Some Computational Aspects of Thinwire Modeling," Lawrence Livermore Laboratory Report, UCRL-74818, June 19, 1973
- 10 Dah-Cheng Kuo, and Straight, B. J., Improved Programs for Analysis of Radiation and Scattering by Configurations of Arbitrarily Bent Thin-Wires, Scientific Report No. 15; 15 January 1972, AFCRL-72-0051, Contract No. F19628-68-C-0180
- 11 Richmond, J. H., "Computer Program for Thin-Wire Structures in a Homogeneous Conducting Medium," NASA Technical Report 2902-12, Grant No. NGL 36-008-138, August 1973

- 12 Rockway, J. W., and Hansen, P. M., "Calculated Near Fields of Navy HF Whip Antennas," NELC Technical Report TR 1872, 24 April 1973
- 13 Landt, J. A., Miller, E. K., and Deadrick, F. J., "Time Domain Computer Models of Thin Wire Antennas and Scatterers," Lawrence Livermore Laboratory Report, UCRL-74848, November 1973
- 14 Blairicum, M. Van, and Miller, E. K., "TWTD: A Computer Program For the Time Domain Analysis of Thin Wire Structures," Lawrence Livermore Laboratory Report, UCRL-51277, October 28, 1972
- 15 Mittra, R., Computer Techniques for Electromagnetics, Pergamon Press Ltd., 1973
- 16 Miller, E. K., "Some Computational Aspects of Transient Electromagnetics," Lawrence Livermore Laboratory Report, UCRL-51276, Contract No. W-7405-Eng-48, AEC, September 19, 1972
- 17 Schelkunoff, S. H., Friis, H. T., Antennas, Theory and Practice, John Wiley & Sons, Inc. 1952
- 18 King, R. W. P., and Harrison, C. W. Jr., Antennas and Waves: A Modern Approach, M.I.T. Press, 1969
- 19 Parsad, S., and King, R. W. P., "Experimental Study of Inverted L-, T-, and Related Transmission-Line Antennas," J. of Research of the National Bureau of Standards - D. Radio Propagation, v. 65D, no. 5, September-October 1961
- 20 Lievens, J. L., and Olson, I. C., "HF Antenna System Design for Patrol Hydrofoil (Missile) (PHM)," NELC Technical Document TD 269, 20 August, 1973
- 21 NAVORD OP 3565/NAVAIR 16-1-529, Hazards of Electromagnetic Radiation to Personnel
- 22 Adams, A. T., and Mendelovicz, E., "The Near-Field Polarization Ellipse," IEEE Transactions on Antennas and Propagation, January 1973
- 23 Everett, W. W., Jr., Adams, A. T., and Perini, J., Topics In Intersystem Compatibility, Holt, Rinehart & Winston, Inc., 1972
- 24 Gustafson, W. E., Chase, W. M., and Poirier, J. H., "Power Absorbed By A Receiving Antenna In Immediate Proximity to Transmitting Antenna," NELC Report 138, NE121008, October 10, 1949
- 25 Lievens, J. L., and DuBrul, D. W., "MLA-I Miniloop Antenna: A Technical Evaluation," NELC Technical Document (to be published)
- 26 Bohley, P., Walter, C. H., and Caldecott, R., "Development of the Multiturn Loop Antenna at HF for Shipboard Applications," Naval Ship Systems Command, Final Report 3518-1, Contract No. N00024-73-C-1023
- 27 NAVELEX 0101, 106, Electro Magnetic Compatibility and Electro Magnetic Radiation Hazards, August 1971

- 28 Lin, J. C., Guy, A. W., and Johnson, C. C., "Power Deposition in a Spherical Model of Man Exposed to 1-20 MHz Electromagnetic Fields," IEEE Transactions on Microwave Theory and Techniques, v. MTT-21, no. 12, December 1973
- 29 Adams, A. T., Straight, B. J., Warren, D. E., Dah-Cheng Kuo, and Baldwin, T. E., "Near Fields of Wire Antennas by Matrix Methods," IEEE Transactions on Antennas and Propagations, v. AP-21, no. 5, September 1973
- 30 Harrison, C. W., "Monopole With Inductive Loading," IEEE Transactions on Antennas and Propagation, v. AP-11, July 1963
- 31 Hansen, R. C., "Optimum Inductive Loading of Short Monopoles," Abstracts of the 23rd Annual Air Force Antenna Symposium, 12 October 1973

## **APPENDIX A: NONRADIATING NETWORK PROGRAM**

This basic computer program calculates the input impedance and dB coupling of a two-port bilateral network.

```

00010      PRINT'
00020      PRINT
00030      PRINT'
00040      PRINT
00050      PRINT'INPUT TWO-PORT ADMITTANCE PARAMETERS Y11,Y12, AND Y22'
00060      INPUT G(1),Y(1),G(2),Y(2),G(3),Y(3)
00070      PRINT'WHAT IS THE OPERATING FREQUENCY IN MHZ'
00080      INPUT F
00090      LET F=F*1000000
00100      PRINT'INPUT LOAD RESISTANCE; INITIAL VALUE; STEP SIZE, NUMBER OF STEPS'
00110      INPUT R8,P1,N
00120      PRINT 'INPUT LOAD REACTANCE; TYPE, INITIAL VALUE, STEP SIZE, NUMBER OF STEPS'
00130      INPUT A,X8,Y1,N
00140      REM 1-MAGNITUDE OF REACTANCE, 2-CAPACITOR, 3-INDUCTOR
00150      R4=R8
00160      PRINT
00170      PRINT
00180      PRINT'TWO-PORT ADMITTANCE PARAMETERS'
00190      PRINT'Y11 = ' G(1) ' + J ' Y(1)
00200      PRINT'Y12 = ' G(2) ' + J ' Y(2)
00210      PRINT 'Y22 = ' G(3) ' + J ' Y(3)
00220      PRINT
00230      PRINT'FREQUENCY = 'F' MHZ '
00240      PRINT
00250      PRINT'R-LOAD','X-LOAD','R-IN','X-IN','RR-COUPLING'
00260      PRINT
00270      FOR J=1 TO N
00280      X4=Y8
00290      FOR I=1 TO M
00300      IF A = 2 THEN 340
00310      IF A = 3 THEN 360
00320      GOTO 390
00330      REM THE REACTIVE COMPONENT IS INDUCTIVE
00340      LET X4 = 2*3.14*F*X8
00350      GOTO 390
00360      REM THE REACTIVE COMPONENT IS CAPACITIVE
00370      LET X4 = -1/(2*3.14*F*X8)
00380      REM USES ADMITTANCE PARAMETERS REPRESENTATION
00390      D1=R4+R4+X4*X4
00400      R=X4/D1
00410      Z1=R+G(3)
00420      Z2=X+Y(3)
00430      Z5=G(2)*G(2)-Y(2)*Y(2)
00440      Z6=2*G(2)*Y(2)
00450      D3=G(2)*G(2)+Y(2)*Y(2)
00460      R2=Z1*Z1+Z2*Z2
00470      Z3=(Z1*Z5+Z2*Z6)/D2
00480      Z4=(Z1*Z6-Z5*Z2)/D2
00490      T=Z3*Z3+Z4*Z4
00500      Y1=G(1)-Z3
00510      Y2=Y(1)-Z4
00520      C1=(R*Y3)/(R2*Y1)
00530      T=Y1*Y1+Y2*Y2
00540      Z5=Y1/T
00550      Z6=-Y2/T
00560      IF C1<1.F-10 GOTO 577
00570      C1=10.0*LOG(C1)
00577      C1=-999.
00580      PRINT R4,X4,Z5,Z6,C1
00590      X4=X4+Y1
00600      NEXT I
00610      R4=R4+R1
00620      NEXT J
00630      PRINT
00640      PRINT'DO YOU WISH TO PROCEED -- 1 FOR YES 0 FOR NO';
00650      INPUT ?
00660      IF ? = 1 THEN 100
00670      END
END OF DATA

```

## APPENDIX B: ARC

A Fortran subroutine for the MBA program, ARC generates the segmentation data for a wire arc located in the X-Z plane.

# WIRE ARC SPECIFICATION (GA)

**PURPOSE:** This card generates a wire arc ( $\leq 360^\circ$ ) of equal segments centered about the origin in the X-Z plane.

**CARD:**

2	5	10	20	30	40	50	60	70	80
GA	ITG	NS	XW1	YW1	ZW1				RAD
The numbers along the top refer to the last column in each field									

**PARAMETERS:**

## INTEGERS

ITG – tag number assigned to wire

NS – number of segments into which arc will be divided

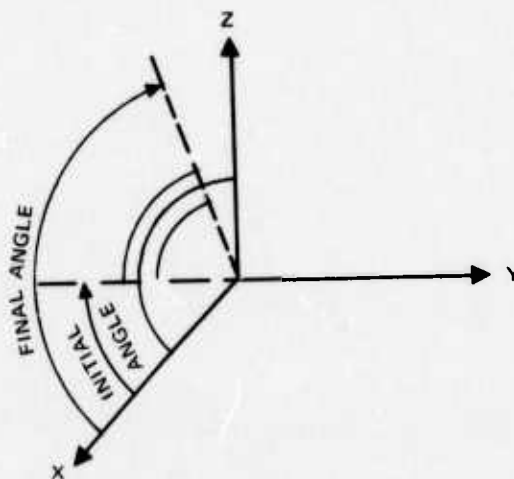
## DECIMAL NUMBERS

XW1 – radius of arc to be generated

YW1 – initial angle of arc in degrees (see diagram below)

ZW1 – final angle of arc in degrees (see diagram below)

RAD – wire radius in same units as arc radius



NOTES:

- The initial and final angles are measured from the X-axis as indicated in the above drawing. Clockwise is the positive sense.
- Wires may not overlap; hence  $|\text{Final Angle} - \text{Initial Angle}| \leq 360^\circ$ . Specification of overlapping wires will terminate the computer run.

```

0001      SUBROUTINE ARC(ITG,NS,RADA,YW1,ZW1,RAD)
          C
          C      SUBROUTINE ARC GENERATES SEGMENT GEOMETRY DATA
          C
0002      IMPLICIT REAL*8 (A-H,O-Z)
0003      COMMON /DAT4/ XI(200),Y(200),Z(200),SI(200),BI(200),ALP(200),
          1 BET(200),ICDN1(200),ICDN2(200),ITAG(200),WLAM,IPSYM,N,NP
0004      DIMENSION X2(1),Y2(1),Z2(1)
0005      EQUIVALENCE (X2(1),SI(1)), (Y2(1),ALP(1)), (Z2(1),BET(1))
0006      IST=N+1
0007      N=N+NS
0008      NP=N
0009      IPSYM=J
0010      IF(NS.LT.1) RETURN
0011      AD=DABS(ZW1-YW1)
0012      IF(AD.GT.360.0) GO TO 20
0013      DEL=YW1*0.0174532925
0014      SAL=AD*0.0174532925/NS
0015      XS1=RADA*DCOS(DEL)
0016      YS1=0.0
0017      ZS1=RADA*DSIN(DEL)
0018      DEL=DEL+SAL
0019      DO 10 I=IST,N
0020      XS2=RADA*DCOS(DEL)
0021      YS2=0.0
0022      ZS2=RADA*DSIN(DEL)
0023      X(I)=XS1
0024      Y(I)=YS1
0025      Z(I)=ZS1
0026      X2(I)=XS2
0027      Y2(I)=YS2
0028      Z2(I)=ZS2
0029      XS1=XS2
0030      YS1=YS2
0031      ZS1=ZS2
0032      BIII=RAD
0033      ITAG(I)=ITG
0034      10 DEL=DEL+SAL
0035      GO TO 30
0036      20 WRITE(6,21)
0037      21 FORMAT('INCORRECT ARC ANGLE SPECIFICATION')
0038      STOP
0039      30 CONTINUE
0040      RETURN
0041      END

```

#### APPENDIX C: NHFLD, HFK, GH

Fortran subroutines for the MBA program calculate the magnetic near fields.



FORTRAN IV G LEVEL 21		HEK	DATE = 74102	20/407
0001		SUBROUTINE HEK(EL1,EL2,RMK,ZPKX,SGR,SGI)		
0002		IMPLICIT REAL*8 (A-H,O-Z)		
0003		COMMON/TMH/ZPK,RMK5		
0004		DATA NX,NM,NTS/1,65536,47,FX/1.0-47		
0005		ZPK=ZPKX		
0006		RMK5=RHK+RMK		
0007		FNH=NM		
0008		Z=EL1		
0009		ZE=EL2		
0010		S=ZE-Z		
0011		FP=S/(10.*FNH)		
0012		ZEND=ZE-FP		
0013		SG=0.0		
0014		SGI=0.0		
0015		NS=NX		
0016		NT=0		
0017		CALL GHEZ,SGR,SGI		
0018	1	FNH=NS		
0019		DX=Z/NS		
0020		DZ=DX*0.500		
0021		ZP=Z+DX		
0022		IF(ZP-ZE).GE.4.5		
0023	5	Z=ZP-Z		
0024		IF(ABS(DZ)-FP).GT.100.100.4		
0025	4	ZP=Z+DZ		
0026		CALL GHEZ,SGR,SGI		
0027		ZP=Z+DX		
0028		CALL GHEZ,SGR,SGI		
0029	23	T00R=(GIR*550)*0.0707		
0030		T00I=(GII*550)*0.0707		
0031		T01R=(T00R+DX*550)*0.500		
0032		T01I=(T00I+DX*550)*0.500		
0033		T10R=(4.0*0.015-T00R)/3.000		
0034		T10I=(4.0*0.015-T00I)/3.000		
0035		T01R=TEST(T01R,T10R)		
0036		T01I=TEST(T01I,T10I)		
0037		IF(T01I-XX).GE.4.5,20		
0038	47	IF(T01I-XX).GE.4.5,20		
0039	21	ZP=Z+DX*0.500		
0040		CALL GHEZ,SGR,SGI		
0041		ZP=Z+DX*0.500		
0042		CALL GHEZ,SGR,SGI		
0043		T02R=(T01R+ZP*(G2I*550)*0.5		
0044		T02I=(T01I+ZP*(G2I*550)*0.5		
0045		T11R=(4.0*0.020-T01R)/3.0		
0046		T11I=(4.0*0.020-T01I)/3.0		
0047		T20R=(16.0*0.015-T11R)/15.0		
0048		T20I=(16.0*0.015-T11I)/15.0		
0049		T02R=TEST(T11R,T20R)		
0050		T02I=TEST(T11I,T20I)		
0051		IF(T02I-XX).GE.4.5,21		
0052	48	IF(T02I-XX).GE.4.5,21		
0053	50	SGR=SGR+T00R		
0054		SGI=SGI+T00I		
0055	60	NT=NT+2		
0056		G1T=52		
0057	51	SGR=SGR+T00R		
0058		SGI=SGI+T00I		

FORTRAN IV G LEVEL 21		HEK	DATE = 74102	20/407
0059	58	NT=NT+1		
0060	52	Z=Z+DX		
0061		IF(Z-ZE).GE.3,100,100		
0062	63	G1R=550		
0063		G1I=550		
0064		IF(NT-NTS).GE.5,5		
0065	54	IF(NT-NTS).GE.5,5		
0066	65	NS=NS/2		
0067		NT=1		
0068		G1T=1		
0069	21	NT=0		
0070		IF(NS-NM).GE.4,5,5		
0071	44	APR=0.001/2		
0072	63	PRMNT(20,1,PT,0,SIZE,LIMIT,AT,ZE,PT,4,5)		
0073		G1T=51		
0074	22	NS=NS*2		
0075		NS=NS		
0076		G1R=550		
0077		DZ=DX*0.5		
0078		NS=550		
0079		G1I=550		
0080		G1R=550		
0081		G1I=550		
0082		G1T=55		
0083	100	G1T=55		
0084		G1R=550		
0085		G1I=550		
0086		G1T=55		
0087		G1T=55		

FORTRAN IV G LEVEL 21

GH

DATE = 74102

```

0001      SUBROUTINE GH(ZK,HR,HI)
0002      IMPLICIT REAL*8 (A-H,O-Z)
0003      COMMON/TMH/ZPK,RKS
0004      RS=ZK-ZPK
0005      RS=2HKS+RS*RS
0006      R=DSQRT(RS)
0007      CKR=DCOS(R)
0008      SKR=DSIN(R)
0009      RP2=1./RS
0010      RR3=RP2/R
0011      HR=SKR*RP2+CKR*RR3
0012      HI=CKR*RP2-SKR*RR3
0013      RETURN
0014      END

```

#### APPENDIX D: HELIX

A Fortran subroutine for the MBA program, HELIX generates the segmentation data for a wire helix.

## WIRE HELIX OR SPIRAL SPECIFICATION (GH)

PURPOSE: This card generates a helix or a spiral around the Z-axis.

CARD:

2	5	10	20	30	40	50	60	70	80
GH	ITG	NS	S	HL	A1	B1	A2	B2	RAD
The numbers along the top refer to the last column in each field.									

PARAMETERS:

### INTEGERS

ITG — tag number

NS — number of segments in the whole helix

### DECIMAL NUMBERS

S — axial spacing between turns

HL — total axial length

A1 — radius in X direction at  $Z = 0$

B1 — radius in Y direction at  $Z = 0$

A2 — radius in X direction at  $Z = |HL|$

$A2 = A1 \rightarrow$  helix,  $A2 \neq A1 \rightarrow$  spiral

Therefore, A2 should not be left blank

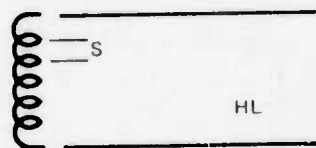
B2 — radius in Y direction at  $Z = |HL|$

RAD — radius of wire

NOTES:

- $B1 = 0$  or left blank  $\rightarrow A1 = B1$
- $B2 = 0$  or left blank  $\rightarrow A2 = B2$
- If  $HL < 0 \rightarrow$  rotation going from top to bottom will be in a counterclockwise direction.  $HL > 0$  rotation is in a clockwise direction.

Also, if  $HL < 0$ , the structure generated is rotated towards the right around the Z axis  $90^\circ$  with respect to the clockwise structure (with  $HL > 0$ ). In other words, A1 will be along the +Y axis and B1 along the +X axis at  $Z = 0$ . To counteract this, add the following card: COORDINATE TRANSFORMATION (GM) -  $90^\circ$ .



```

0001 SUBROUTINE HELIX(S,HL,A1,B1,A2,B2,RAD,NS,ITG)
      C SUBROUTINE HELIX GENERATES SEGMENT GEOMETRY DATA FOR A HELIX OF NS
      C SEGMENTS
0002 (IMPLICIT REAL*8(A-H,I-Z))
0003 COMMON /DATA/ X(200),Y(200),Z(200),S1(200),B1(200),ALP(200),
      1 BET(200),ICON1(200),ICON2(200),ITAG(200),WLAM,IPSYM,N,NP
0004 DIMENSION X2(1),Y2(1),Z2(1)
0005 EQUIVALENCE (X2(1),S1(1)), (Y2(1),ALP(1)), (Z2(1),BET(1))
0006 DATA PI/3.1415926535/
0007 (ST=N+1
0008 N=N+NS
0009 NP=N
0010 IPSYM=0
0011 IF(NS.LT.1) RETURN
0012 TURNS=2ABS(HL/S)
0013 ZINC=DABS(HL/NS)
0014 Z(1)=0
0015 DO 25 I=1,ST,N
0016 B1(I)=RAD
0017 ITAG(I)=ITG
0018 IF(I.NE.1) Z(1)=Z(1-1)+ZINC
0019 Z2(1)=Z(1)+ZINC
0020 IF(A2.NE.A1) GO TO 10
0021 IF(B1.EQ.0) A1=A1
0022 X(1)=A1*DCOS(2.00*PI*Z(1)/S)
0023 Y(1)=B1*DSIN(2.00*PI*Z(1)/S)
0024 X2(1)=A1*DCOS(2.00*PI*Z2(1)/S)
0025 Y2(1)=B1*DSIN(2.00*PI*Z2(1)/S)
0026 GO TO 20
0027 10 IF(B2.EQ.0) B2=B2
0028 X(1)=(A1+(A2-A1)*Z(1)/DABS(HL))*DCOS(2.00*PI*Z(1)/S)
0029 Y(1)=(B1+(B2-B1)*Z(1)/DABS(HL))*DSIN(2.00*PI*Z(1)/S)
0030 X2(1)=(A1+(A2-A1)*Z2(1)/DABS(HL))*DCOS(2.00*PI*Z2(1)/S)
0031 Y2(1)=(B1+(B2-B1)*Z2(1)/DABS(HL))*DSIN(2.00*PI*Z2(1)/S)
0032 20 IF(HL.GT.0) GO TO 25
0033 COPY=X(1)
0034 X(1)=Y(1)
0035 Y(1)=COPY
0036 COPY=X2(1)
0037 X2(1)=Y2(1)
0038 Y2(1)=COPY
0039 25 CONTINUE
0040 IF(A2.EQ.A1) GO TO 21
0041 SANGLE=DATAN(A2/(DABS(HL)+(DABS(HL)*A1)/(A2-A1)))
0042 WRITE(6,104)SANGLE
0043 104 FORMAT(5X,'THE CONE ANGLE OF THE SPIRAL IS',F10.4)
0044 RETURN
0045 21 IF(A1.NE.B1) GO TO 30
0046 H01A=2.00*PI
0047 TURN=H01A*PI
0048 GO TO 40
0049 30 IF(A1.LT.B1) GO TO 34
0050 H44A=2.00*A1
0051 H41A=2.00*B1
0052 GO TO 35
0053 34 H44A=2.00*B1
0054 H41A=2.00*A1
0055 35 H01A=DSORT((H44A**2+(H41A**2)/2**H41A)

```

```

0056 TURN=2.00*PI*H01A
0057 40 PITCH=DATAN(S/PI*H01A)
0058 WRITE(6,105)PITCH,TURN
0059 105 FORMAT(5X,'THE PITCH ANGLE IS',F10.4/5X,'THE LENGTH OF WIRE/TURN IS',F10.4)
0060 RETURN
0061 END

```

# INITIAL DISTRIBUTION LIST

## CHIEF OF NAVAL MATERIAL

MAT 031

## COMMANDER, NAVAL SEA SYSTEMS COMMAND

06T

LIBRARY

## COMMANDER, NAVAL ELECTRONIC SYSTEMS COMMAND

ELEX 03

ELEX 31031 (4)

ELEX 5012

ELEX 51012

ELEX 094

ELEX 501

ELEX 5103

ELEX 5401

ELEX PME 121

ELEX PME 117

LIBRARY

## COMMANDER, NAVAL SHIP ENGINEERING CENTER

CODE 6174

CODE 6179

CODE 6179C03 (4)

## CHIEF OF NAVAL OPERATIONS

OP-098T

OP-098

OP-093

OP-094

OP-941

OP-986

## CHIEF OF NAVAL RESEARCH

CODE 406

CODE 427

## COMMANDER IN CHIEF

PACIFIC FLEET

ATLANTIC FLEET

## COMMANDER, NAVAL TELECOMMUNICATIONS COMMAND

NTSA

## COMMANDANT, U.S. COAST GUARD HO

## U.S. COAST GUARD ELECTRONIC

ENGINEERING CENTER, WILDWOOD, N.J.

## ASST SECRETARY OF THE NAVY

(RESEARCH AND DEVELOPMENT)

## NAVAL SECURITY GROUP HEADQUARTERS

LIBRARY

## INSTITUTE OF NAVAL STUDIES

LIBRARY

## DEFENSE DOCUMENTATION CENTER (2)

## DOD RESEARCH AND ENGINEERING

TECHNICAL LIBRARY

ASSISTANT DIRECTOR

(COMMUNICATIONS & ELECTRONICS)

## FEDERAL AVIATION AGENCY

SYSTEMS RESEARCH & DEVELOPMENT SERVICE

## DEFENSE COMMUNICATIONS AGENCY

## ENVIRONMENTAL SCIENTIFIC SERVICE ADM/INSTITUTE

FOR TELECOMMUNICATION SCIENCES & AERONOMY,  
BOULDER, COLORADO

LIBRARY

## ELECTROMAGNETIC COMPATIBILITY ANALYSIS CENTER

## ARMY ELECTRONICS RESEARCH & DEVELOPMENT LAB.

## ARMY RESEARCH OFFICE (DURHAM)

CRD-AA-1P

## ARMY ELECTRONIC WARFARE LABORATORY

MOUNTAIN VIEW OFFICE

## FORT HUACHUCA

52D USASASOC

## AIR FORCE HEADQUARTERS

DIRECTOR OF COMMAND CONTROL & COMMUNICATIONS

## NAVAL AIR DEVELOPMENT CENTER

NADC LIBRARY

## NAVAL UNDERWATER SYSTEMS CENTER

LIBRARY

## NAVAL RESEARCH LABORATORY

LIBRARY

## NAVAL POSTGRADUATE SCHOOL

LIBRARY

CODE 52 - R. ADLER

## OFFICE OF NAVAL RESEARCH BRANCH OFFICE

BOSTON

CHICAGO

LONDON

PASADENA (CHIEF SCIENTIST)

## ROME AIR DEVELOPMENT CENTER

EMLAL-1 (DOCUMENT LIBRARY)

## MARINE CORPS HEADQUARTERS

LIBRARY